Update on the Simulation of Commercial Drying of Spent Nuclear Fuel

Spent Fuel and Waste Disposition

Prepared for
US Department of Energy
Spent Fuel and Waste Science and Technology

S.G. Durbin, E.R. Lindgren, R.J.M. Pulido, A. Salazar III, R.E. Fasano

Sandia National Laboratories

September 23, 2021

Milestone No. M2SF-21SN010203033

SAND2021-XXXX R

Prepared by
Sandia National Laboratories
Albuquerque, New Mexico 87185 and Livermore, California 94550

Sandia National Laboratories is a multimission laboratory managed and operated by National Technology and Engineering Solutions of Sandia, LLC, a wholly owned subsidiary of Honeywell International, Inc., for the U.S. Department of Energy's National Nuclear Security Administration under contract DE-NA0003525.

ABSTRACT

The purpose of this report is to document improvements in the simulation of commercial vacuum drying procedures at the Nuclear Energy Work Complex at Sandia National Laboratories.

Validation of the extent of water removal in a dry spent nuclear fuel storage system based on drying procedures used at nuclear power plants is needed to close existing technical gaps. Operational conditions leading to incomplete drying may have potential impacts on the fuel, cladding, and other components in the system. A general lack of data suitable for model validation of commercial nuclear canister drying processes necessitates additional, well-designed investigations of drying process efficacy and water retention. Scaled tests that incorporate relevant physics and well-controlled boundary conditions are essential to provide insight and guidance to the simulation of prototypic systems undergoing drying processes.

This report documents a new test apparatus constructed at a reduced scale with multiple PWR fuel rod surrogates and a single guide tube dashpot. This apparatus is fashioned from a truncated 5×5 section of a prototypic 17×17 PWR fuel skeleton and includes the lowest segment of a single guide tube, often referred to as the dashpot region. The guide tube in this assembly is open and allows for insertion of a poison rod (neutron absorber) surrogate. A drying procedure was developed based on measurements from the process used for the High Burnup Demonstration Project. This test procedure consisted of filling the externally-heated pressure vessel with water, draining the water with gravity and multiple helium blowdowns, evacuating additional water with a vacuum drying sequence at successively lower pressures, and backfilling with helium.

Results indicate that after bulk water is removed from the pressure vessel, residual water is verifiably measured through confirmatory measurements of pressure and water content using a mass spectrometer. The apparatus was tested with an empty guide tube and a guide tube with a poison rod inserted. The final pressure rebound behavior was well below the established regulatory limit of less than 0.4 kPa (3 Torr) within 30 minutes of isolation.

The operational and analytical experiences gained from this test series allow for focus on the dashpot region of the fuel assembly and will guide the transition to full assembly-scale tests at prototypic length. A planned, full-length assembly represents the next evolutionary step in this test series and will feature prototypic assembly hardware, failed fuel rod simulators with engineered cladding defects, and guide tubes with obstructed dashpots to challenge the drying system with multiple retention sites.

This page is intentionally left blank.

ACKNOWLEDGEMENTS

The authors would like to acknowledge the hard work and commitment of all contributors to the project. In particular, we would like to acknowledge the strong support and leadership of Ned Larson at the Department of Energy. Sylvia Saltzstein (SNL) and Geoff Freeze (SNL) are to be commended for their programmatic and technical guidance.

We would like to express our gratitude for the hard work and dedication of our technologists Greg Koenig, Ronald Williams III, Adrian Perales, Beau Baigas, and Gregory Thad Vice that made the success of this project possible.

This page is intentionally left blank.

CONTENTS

LIST OF FIGURES

LIST OF TABLES

This page is intentionally left blank.

EXECUTIVE SUMMARY

Technical gaps exist in the understanding of the extent of water removal in a dry spent nuclear fuel storage system with commercial canister drying procedures (Hanson & Alsaed, 2019). Operational conditions leading to substantial amounts of residual water may have potential impacts on the fuel, cladding, and other components in the system, such as fuel degradation and cladding corrosion, embrittlement, and breaching. Additional information is needed on drying process efficacy to evaluate the potential impacts of water retention on long-term dry storage. Given the lack of data suitable for the model validation of drying processes, carefully designed investigations that incorporate relevant physics and well-controlled boundary conditions are needed to supplement existing field data. Experimental components, methodology, and instrumentation are therefore under development for use in advanced studies of realistic drying operations conducted on surrogate spent nuclear fuel.

A small-scale pressure vessel was devised that incorporated a truncated sub-assembly of prototypic pressurized water reactor (PWR) hardware to demonstrate operational capabilities and the utilization of moisture monitoring equipment during drying processes as shown in Figure E-1. The Dashpot Drying Apparatus (DDA) consists of the truncated fuel assembly, a pressure/vacuum vessel, and external heaters to simulate decay heat. A drying procedure was devised to investigate the efficacy of residual water removal after introduction and draining of water from the pressure vessel. A mass spectrometer (MS) with specially designed inlets ("HPR-30") was used to monitor moisture and gas composition at various pressure ranges, while other water removal behavior was deduced from pressure and temperature measurements.

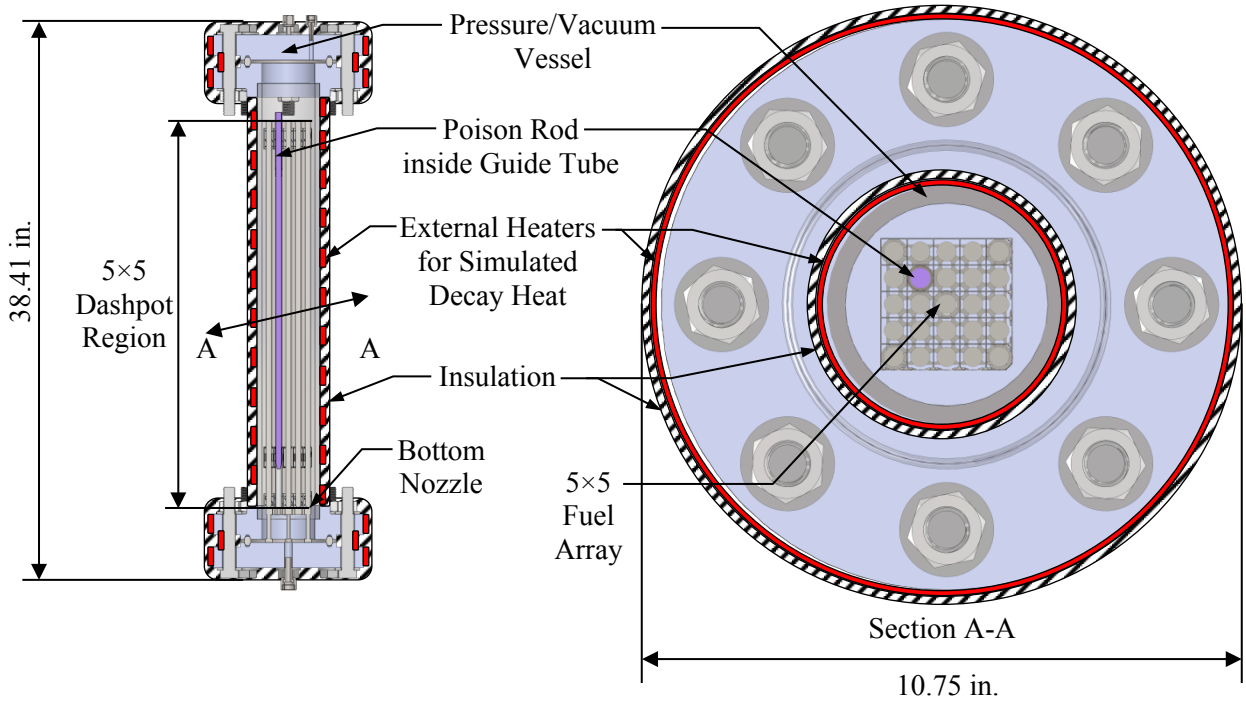

Figure E-1 Major components of the Dashpot Drying Apparatus.

A metered amount of water was introduced into the pressure vessel, drained by gravity, and then subjected to multiple blowdowns with helium from 160 kPa to 100 kPa. Afterwards, vacuum drying was performed by implementing sequential hold points at increasingly lower pressures from 50 kPa (380 Torr) to below 0.01 kPa (0.1 Torr) and monitoring the change in pressure as the system was isolated from the vacuum pump. At the final and lowest pressure, the isolated system pressure was not to exceed 0.4 kPa (3

Torr) after 30 minutes in the final hold in accordance with the regulatory criterion for dryness. These tests were conducted under externally-heated conditions with two types of water-retaining assembly configurations: 1) an empty guide tube, and 2) a guide tube with a poison rod inserted. The poison rod is a component with neutron-absorbing material that allows for criticality control in a nuclear reactor. The presence of the poison rod surrogate introduces an annular gap and is intended to represent a water retention site as would be observed in a prototypic system.

Figure E-2 shows the bottom-most guide tube temperature and system pressure during the drying test for a dashpot with an inserted poison rod. During the vacuum drying process, the sudden decrease in temperature after $t = 4.03$ hours indicates that liquid water was initially present during the 10 kPa (76 Torr) hold. Afterwards, the temperature eventually rises and stabilizes when the system is brought to lower vacuum hold points and the final helium backfill.

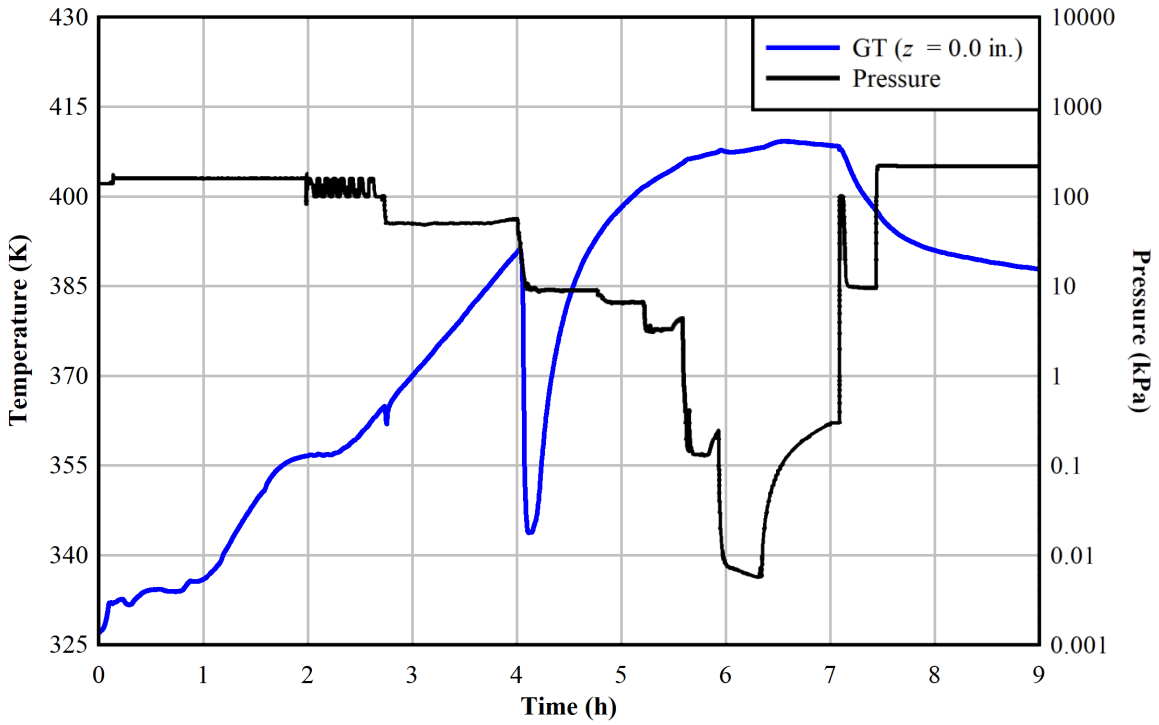

Figure E-2 Bottom-most guide tube (GT) temperature and system pressure during the 8/25/21 drying test.

Bulk water was observed to be largely removed in post-test mass measurements with loss on the order of ~50 – 150 grams (~0.1 – 0.3 pounds). Gas composition data was obtained by the mass spectrometer during the final hold points of the test and a series of additional vacuum isolation holds (at approximately 10 kPa) and subsequent helium re-pressurizations to 220 kPa. These measurements confirmed a reduction in water content over time.

Results indicate satisfactory drying operation of the DDA and successful implementation of moisture monitoring equipment. The data and operational experience from these tests will guide the next evolution of experiments on a prototypic-length scale with multiple surrogate rods in a full 17×17 PWR assembly. This assembly will feature partially submersible heater rods and a specialized test rod to introduce specialized water retention sites and internal rod pressure monitoring. The insight gained through these investigations is expected to support the technical basis for the continued safe storage of SNF into long term operations.

ACRONYMS / ABBREVIATIONS

ADCS	Advanced Drying Cycle Simulator
DAQ	data acquisition system
DDA	Dashpot Drying Apparatus
DOE	Department of Energy
EPRI	Electric Power Research Institute
FHD	forced helium dehydration
FS	full-scale
GT	guide tube
HBDP	High Burnup Demonstration Project
ID	inner diameter
ISFSI	Interim Spent Fuel Storage Installation
MS	mass spectrometer
NIST	National Institute of Standards and Technology
OD	outer diameter
ppmv	parts per million by volume
PV	pressure vessel
PWR	pressurized water reactor
SCR	silicon-controlled rectifier
SNF	spent nuclear fuel
SNL	Sandia National Laboratories
SFWD	Spent Fuel and Waste Disposition
TC	thermocouple
VCR	vacuum coupling radiation
WVIA	water vapor isotope analyzer

This page is intentionally left blank.

UPDATE ON THE SIMULATION OF COMMERCIAL DRYING OF SPENT NUCLEAR FUEL

This report fulfills milestone report M2SF-21SN010203033 in the Spent Fuel and Waste Science and Technology (SFWST) work package (SF-21SN01020303). This work was sponsored under the Department of Energy's (DOE) Office of Nuclear Energy (NE) Spent Fuel and Waste Disposition (SFWD) campaign.

1 INTRODUCTION

1.1 Objective

Numerous water retention sites may exist within the internal volume of a multi-assembly dry storage system that require a specialized approach for the evacuation of water. While guidelines exist on ensuring sufficient evacuation of water from assembly cavities, there is a lack of time-dependent data on water removal from full-scale commercial drying procedures. Obtaining such data has been identified as a high-priority research topic to advance the technical basis for the long-term management of spent nuclear fuel (SNF) (Hanson and Alsaed, 2019). Operational conditions leading to incomplete drying may have potential impacts on the fuel, cladding, and other components in the system.

Drying procedures have been simulated in the laboratory (Colburn, 2021; Knight, 2019) and data has been obtained from samples of canisters subjected to commercial drying processes (Bryan *et al.*, 2019). While transient vacuum drying data has been analyzed for a small-scale apparatus in previous studies at SNL (Salazar *et al.*, 2020), additional information is needed to evaluate the potential impacts of water retention on extended long-term dry storage for a commercial cask system. This includes unique locations in prototypic fuel assembly and canister hardware where water may be more difficult to remove, such as dashpots. Direct measurement of residual water in scaled systems representative of commercial systems is therefore necessary to advance the current technical understanding of the drying procedures used by industry.

This report documents tests conducted on a truncated PWR sub-assembly that incorporates several important prototypic geometries that will be present in the full-length assembly tests to be conducted in the near future. This chapter will discuss the motivating issues underlying the investigation and a summary of past tests that were designed to respond to some of these concerns. Chapter 2 will discuss development of the instrumentation, equipment, and procedures for the test series, including moisture-monitoring equipment. Chapter 3 will discuss the results of the tests, while Chapter 4 will summarize the findings of the investigation and discuss future work.

1.2 Prototypic Thermal-Hydraulics

Prototypic hardware is incorporated to mimic the important geometries found in dry storage systems. One goal of this testing is to preserve actual fuel assembly geometry and associated retention sites for residual water.

Figure 1-1 shows locations within a PWR fuel assembly that can serve as water retention sites, such as the mixing vanes and bulge joints of the grid spacers. The fuel assembly features guide thimble tubes for the insertion of control rods or burnable poison assemblies which function as neutron absorbers for criticality control in the reactor. The dashpots in the guide tubes are designed to drain water through a centrally located through-hole in the guide thimble bolt (i.e. vent hole). If the vent hole is fouled during reactor operations or pool storage, the dashpot could conceivably retain bulk water during the initial draining operations preceding canister drying. However, the water would be free to communicate with the interior of the canister via the flow holes and the open top of the guide thimble during drying operations. Burnable poison rods are inserted and left in some fuel assemblies, which could restrict the flow area for any trapped water in the dashpot region if the vent hole is fouled.

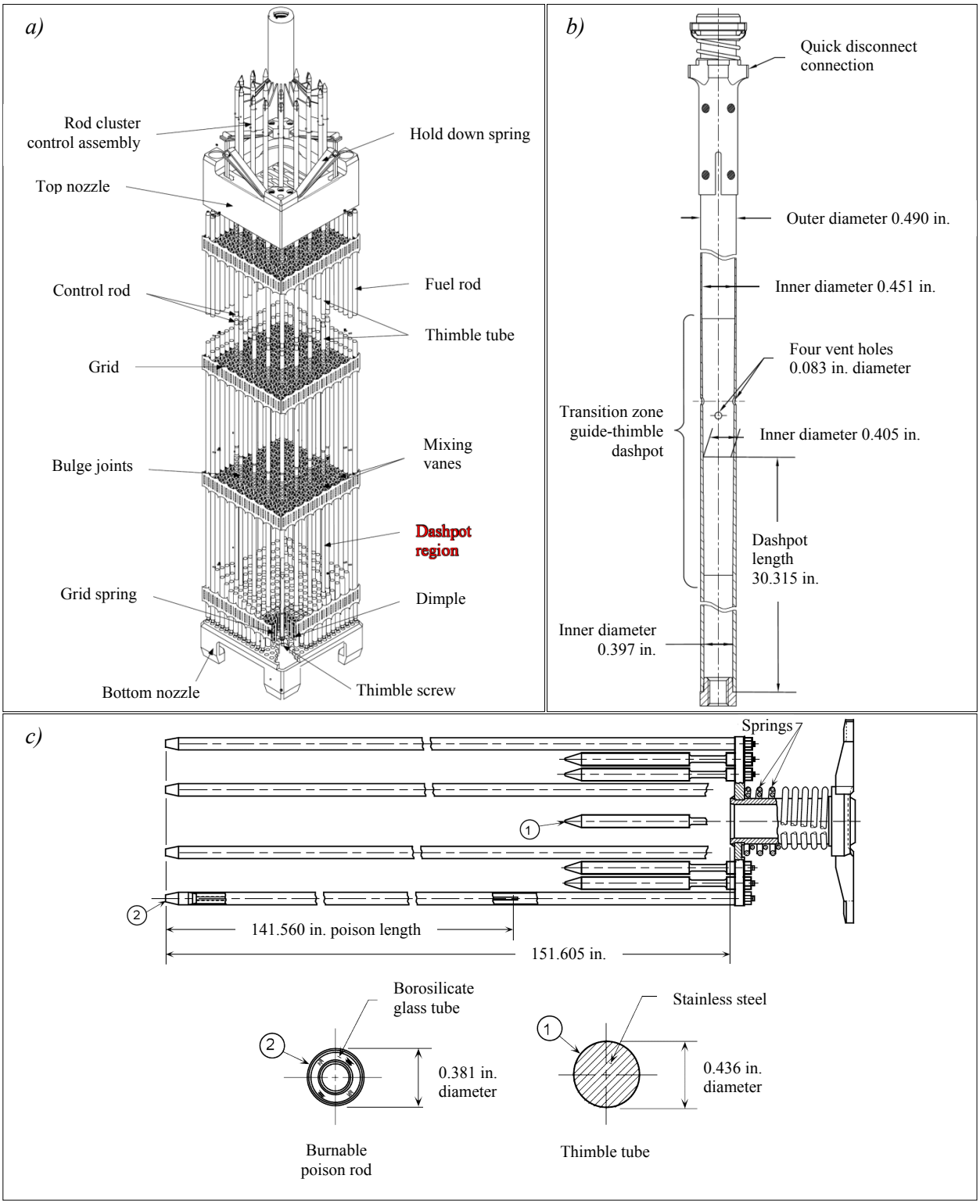

Figure 1-1 Water retention sites exhibited in *a)* a typical 17×17 PWR fuel assembly construction, *b)* a typical PWR guide thimble tube, and *c)* a burnable poison rod assembly (Figures 3.1-16, 4.2-8, and 3.1-26 in NRC, 2002).

1.3 Residual Water

Spent fuel assemblies are dried after interim storage in pools to ensure the removal of water in assembly cavities as a defense against issues related to pressurization and corrosion that might occur during the subsequent, potentially long-term, dry storage process. The evacuation of most water and oxidizing agents contained within the canister is recommended by NUREG-1536 (NRC, 2010). A pressure of 0.4 kPa (3 Torr) is recommended to be held in the canister for at least 30 minutes while isolated from active vacuum pumping as a measure of sufficient dryness in the canister. A similar drying method developed at Pacific Northwest National Laboratory (PNNL) is suggested (Knoll & Gilbert, 1987), where less than 0.25 volume percent (2500 ppm_v) of oxidizing gases are left in the canister (1 mole in 7 m^3 at 150 kPa and 300 K).

An industry standard guide was established for the drying of SNF after cooling in spent fuel pools (ASTM, 2016). The main purpose of the standard is to aid in the selection of a drying system and a means of ensuring that adequate dryness is attained. Examples of typical commercial processes are documented in the standard, where there is adherence to the aforementioned 0.4 kPa (3 Torr) level when discussing the measurement of pressure rebounds. However, there are no substantial details on the utilization of moisture content measurements to ensure adequate water removal, and the establishment of related dryness metrics are deferred to regulatory agencies. There is only a broad recommendation to impose drying conditions that maximize moisture removal from the system.

Water remaining in canisters upon completion of vacuum drying can lead to corrosion of cladding and fuel, embrittlement, and breaching. There is also some risk of creating a flammable environment from free hydrogen and oxygen generated via the radiolysis of water. The remnant water may be chemically absorbed (chemisorbed), physically absorbed (physisorbed), frozen, or otherwise trapped in cavities, blocked vents, breached clads, damaged fuel, etc. Chemisorbed water is bound to components by forces equivalent to a chemical bond, such as the formation of hydroxides and hydrates on zirconium, or corrosion products on the fuel or cladding. Physisorbed water is bound to components by weaker forces (e.g. Van der Waals, capillary) as an adsorbate, and increased surface area provided by material defects enhances this effect.

The removal of unbound water is largely dependent on the geometry and tortuosity of the components and the speed of the drying process. Cladding breaches are notable cases in that water can become trapped inside a fuel rod between fuel pellets and absorbed in cracks and voids. Water vapor may continue to be diffusively released after vacuuming. Depending on the thermal profile, condensation may occur on the cooler surfaces of the canister and internal hardware, such as those lying at the lower extremes distant from heat emitting SNF.

The pressure applied during vacuum drying lies below the water vapor pressure. Given the unique heat retention and phase change properties of water, when significant heat is removed during volatilization, some quantity of liquid may freeze (ASTM, 2016) and inhibit water removal. It is therefore important to understand under what marginal conditions ice may form during the procedure. Careful control of the vacuum pumps may prevent ice formation by controlling suction near pressures liable to introduce liquid-to-solid phase transitions. Further mitigation may be achieved by implementing pressure reduction in stages that involve bringing the temperature to equilibrium with hot inert gases like helium prior to commencement of the next stage. In a general expansion of this concept, further research and development on forced helium dehydration (FHD) has been recommended to address recently identified technological gaps (Hanson & Alsaed, 2019).

If vacuum is employed to remove water from a canister, measurements in the pressure response to intermittent pump operation may serve as a good indicator of residual, unbound water (ASTM, 2016). Such an approach would involve analysis of the time-dependent pressure rebound when the vacuum pump is isolated from the system. The system is considered adequately dry if the system pressure remains below 0.4 kPa (3 Torr) for at least 30 minutes. Monitoring the moisture content in gas removed from the canister

is also suggested as a means of evaluating adequate dryness. Dew point monitoring and spectroscopic techniques could be used to this end, although these measurements must be benchmarked to understand how they scale to various levels of dryness.

1.4 High Burnup Demonstration

The High Burnup Demonstration Project (HBDP) spent fuel data project from the DOE SFWST program is an ongoing research platform to examine the performance of high burnup spent nuclear fuel in dry storage systems. The project included the loading, drying, and storage of an Orano TN-32B at the Independent Spent Fuel Storage Installation (ISFSI) at the North Anna Nuclear Power Station in Virginia.

1.4.1 Transient Vacuum Drying Data

Data are available on the drying procedures employed in the transfer of the assemblies to the decontamination bay and subsequent loading into the TN-32B (EPRI, 2019) along with STAR-CCM+ and COBRA-SFS model validation (J. Fort *et al*., 2019). These data include ambient temperatures at the facilities, cask surface temperatures, and fuel temperatures, along with additional measurements for long-term cask monitoring. Of particular importance to this report are the data obtained and analyzed for the transients observed during the loading and vacuum drying processes. That is, time-dependent measurements from the HBDP are poised to inform the test setup for this scaled demonstration with prototypic hardware.

The SNF within the TN-32B was put through a prototypic loading and drying process with some minor exceptions involving the installation of instrumentation. The process proceeded as follows:

1. Loading of SNF assemblies from the spent fuel pool into the submerged cask.
2. Movement of the cask into the decontamination bay and installation of the draining and drying equipment.
3. Drainage of the cask using helium as a cover gas.
4. Multiple blowdowns of the cask until bulk flow of liquid water was visually observed to cease.
5. Vacuum drying of the cask using successive stages of increasingly low pressures until the pressure was observed to not exceed 3 Torr within 30 minutes when the cask was isolated.
6. Backfilling of the canister with helium to 222 kPa (1665 Torr).

For the scaled test, the simulation capability of the experimental apparatus can accommodate water filling (representing the cask loading within the pool and the transfer period), drainage, blowdown, vacuum drying, and backfilling. Table 1-1 shows the elapsed times for major events during the HBDP drying processes starting with the beginning of the water draining. This sequence of events, and the resulting temperatures and pressures in the fuel and cask, sets the values for which the DDA tests were conducted to replicate.

The peak measured temperature during vacuum drying was 237 °C, which occurred at the center of the cask slightly above the mid-plane eight hours after the start of vacuum drying (EPRI, 2019). Due to the offset of the thermocouple lance, this maximum implied a peak cladding temperature of 240 °C, which is well below the regulatory limit of 400 °C. The maximum steady-state measurement of 231 °C was obtained during the helium backfill. The maximum external cask surface temperature was 88.3 °C near the cask midplane as measured 12 days after the backfill with helium.

Table 1-1 Elapsed times for the TN-32B water removal and backfill procedures from the HBDP (EPRI, 2019).

Procedure	Elapsed Time (h)
Begin drain	0.00
Finish drain	0.72
Begin blowdowns	4.63
Finish blowdowns	7.18
Begin vacuum drying	7.22
Vacuum drying complete	14.31
Begin initial helium backfill	15.63
Begin final helium backfill	16.22
Finish backfill	17.03

1.4.2 Gas Sampling

Prior to transportation to the ISFSI, samples of the helium backfill gas were collected at 5 hours, 5 days, and 12 days after the drying process (Bryan *et al.*, 2019). Samples were obtained in 1 L cylinders pressurized to 20 psig. Gas samples were analyzed first at room temperature by Dominion Energy using a gas chromatograph. They were then re-analyzed in a more thorough manner with heating at SNL to mitigate sorption effects in the sample bottles. Mass spectrometry was used to quantify bulk and trace gases in the sample while a humidity sensor was used to measure water content.

The Dominion water content analysis employed a Los Gatos Research Water Vapor Isotope Analyzer (WVIA). The instrument is designed for ambient vapor analysis in the field using an absorption technique with an optical cavity measurement cell. Although it operates best with a continuous flow stream, the North Anna cask could not be sampled directly as a failure scenario would result in a release pathway to the decontamination bay. Therefore, the static samples were employed instead and analyzed continuously while connected to the WVIA. The measured water content was 1633, 8896, and 8300 ppm_v for samples 1-3, respectively.

The mass spectrometer employed in the SNL analysis was a Finnigan MAT 271 high-resolution MS specialized for hydrogen isotope measurements via a stable gas ionization source. The instrument employs a combination Faraday cup and secondary electron multiplier for measurement of bulk and trace gases, respectively, and it was calibrated using a precision gas mixture. Measurements were obtained with a 50 cm^3 sample cylinder in line with a high vacuum system using an established high-purity sample and measurement procedure. Water was able to be measured, but its content was underestimated when present as a trace gas and overestimated when present in higher concentrations. Therefore, only estimates of the water content could be provided by the MS due to sorption effects in the sample chamber. However, valuable insight was gained on radiolysis and the formation of anoxic corrosion byproducts and hydrogen gas. Also, no fission gases were detected in the analyses, indicating a lack of fuel failure during cask loading.

The ultimate sensor used for water content measurement at SNL was a Vaisala model HMP77B relative humidity probe mounted to the sample bottle on a tee with a pressure gauge. With an operating range of -70 °C to 180 °C, the probe could be placed directly in an oven during sample heating. It was also capable of static measurements but valves in the vacuum line required some period of time for the system to re-settle for a given adjustment. Measurements were obtained at temperatures ramping up to 65 °C. Water content was found to be 10000 $ppm_v \pm 1000$ ppm_v and 17400 $ppm_v \pm 1740$ ppm_v five and twelve days after drying, respectively, ultimately indicating that 100 grams of water remained in the gas phase in the cask. (The measurements of the 5-hour sample were affected by a leak, but the room temperature measurement was 2097 ppm_v). However, because the relative humidity was less than the anticipated 10%

at 85 °C at the time of sampling, no liquid water was found to exist within the canister unless trapped in locations inaccessible to the drying system.

Given the method of sampling from the HBDP, it may not be possible to implement an MS or humidity probe in a canister with live SNF. Regulatory guidelines present limitations in the type of data that can be obtained in a commercial system. For example, it may not be possible to sample gas for mass spectrometry from the vacuum drying process using a slip stream.

1.4.3 Scaled Demonstration

Figure 1-2 shows a conceptual vertical cross-sections through the HBDP cask and the DDA. Figure 1-2a on the left is adapted from Figure 1.2-1 in TN-32 Final Safety Analysis Report (FSAR), Revision 2. Figure 1-2b on the right shows the DDA. The DDA is designed to represent one dashpot from a single fuel assembly surrounded by a 5×5 fuel array and will be described in detail in Chapter 2.

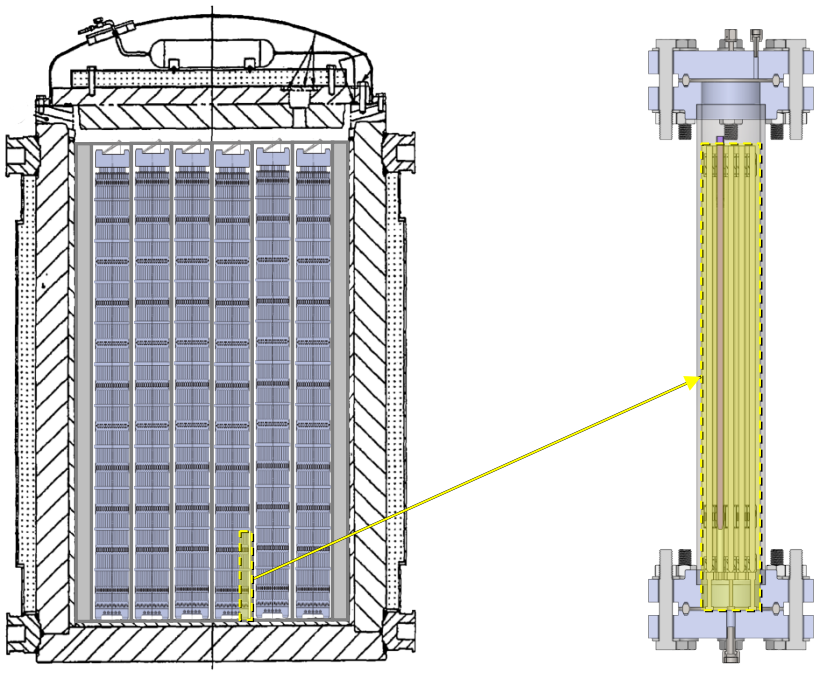

(a) *(b)*

Figure 1-2 Cross-sections showing a) portion of fuel from the High Burnup Demonstration Test represented by b) the Dashpot Drying Apparatus.

2 DEVELOPMENT AND TESTING

This chapter will discuss the testing setup and methodology that aims to address gaps in the current understanding of vacuum drying and residual water analysis that were previously covered in SAND2020-5341 R, "Development of Mockups and Instrumentation for Spent Fuel Drying Tests," (Salazar *et al.*, 2020) and SAND2019-11281 R, "Advanced Concepts for Dry Storage Cask Thermal-Hydraulic Testing" (Salazar *et al.*, 2019).

2.1 Test Objectives

Tests were conducted to verify the removal of residual water in a stainless-steel pressure vessel (4.5 inch OD, 3.826 inch ID) with an integrated prototypic dashpot and removeable poison rod as potential water retention sites in the DDA system. This system allows for thermal-hydraulic investigations of drying efficiency with prototypic hardware.

The main objectives of the test include the following:

1. Demonstrate that a drying procedure can be implemented to remove water retained in the pressure vessel, where pressure measurements can confirm minimal rebound pressures after the application of several vacuum hold points
2. Refine procedures and provide diagnostics for system equipment and moisture monitoring instrumentation, in particular the use of mass spectrometry

Performance verification in this test series with the DDA will support more advanced drying tests employing heater rods and specialized rods in a full-size assembly. In turn, data can be provided that are readily scalable to commercial dry cask storage and transportation applications.

2.2 Fuel Assembly

The PWR sub-assembly was harvested by cutting out a 5×5 section from one corner of a 17×17 PWR skeleton, which included one guide tube dashpot attached to the lowest grid spacer and the debris catcher. The concept is shown in Figure 2-1, and a photo of the assembly is shown in Figure 2-2.

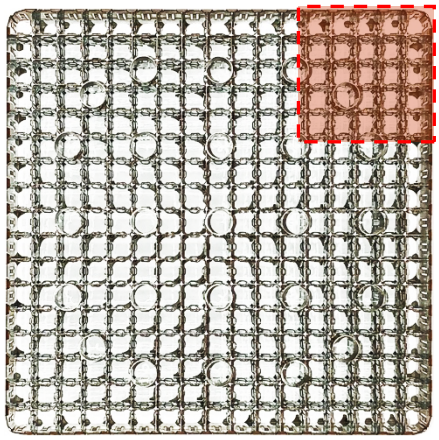

Figure 2-1 Concept for taking 5×5 subassemblies from a 17×17 PWR skeleton. The sub-assembly placed in the pressure vessel was taken from one of the corners (red).

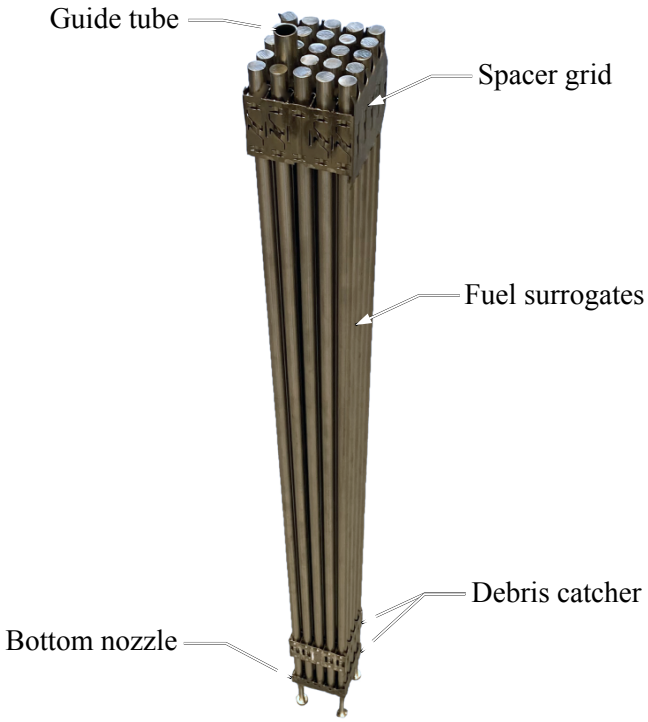

Figure 2-2 Photo of the 5×5 sub-assembly. The guide tube was fitted with a surrogate poison rod for some tests.

The rod layout for the sub-assembly is shown in Figure 2-3. Fuel rod surrogates were placed in the locations in the assembly labeled in red. The vacuum drying procedure was tested twice, with the two tests distinguished by either the inclusion or the absence of a 304 stainless-steel rod that serves as a geometrically prototypic surrogate poison rod. This poison rod was placed in the guide tube location as indicated in Figure 2-3. Additional details of the fuel rod, guide tube, poison rod and assembly are shown in Figures A-Figure A-1 through A-Figure A-5 in Appendix A.

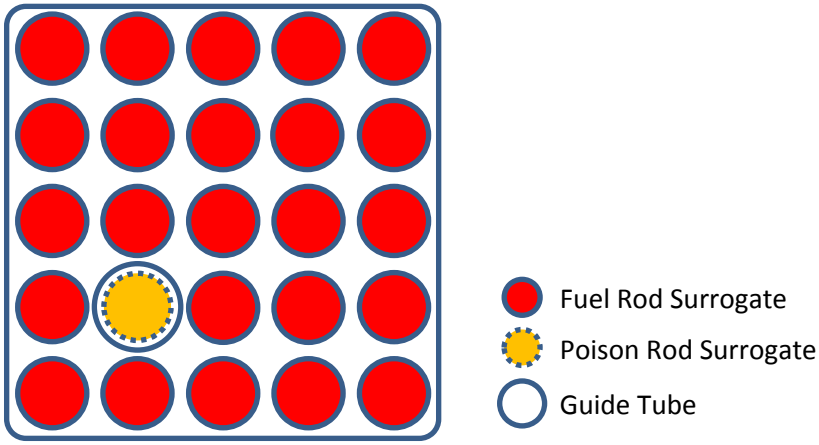

Figure 2-3 Rod layout for a 5×5 mini-assembly.

2.3 Pressure Vessel and Test Setup

A pressure vessel (PV) was constructed of nominal four-inch 316 stainless-steel schedule 80 pipe terminated with welded flanges. The flanges are connected to blinds by ring-type joints (RTJ).

Penetrations into the PV are made via welded glands with vacuum coupling radiation (VCR) face seal connections. A photo of the pressure vessel is shown in Figure 2-4, and a photo of the complete test setup is shown in Figure 2-5. A schematic of the PV is also shown in Figure A-6 in Appendix A.

All VCR connections are sealed with unplated, non-retaining stainless-steel gaskets. Leak testing was conducted using the leak test ports on the female VCR nuts and measuring increases in pressure in the evacuated system. The mass spectrometer was also employed as a helium leak testing method, where a background helium concentration was measured first and then analyzed for spikes when testing a given port.

The top and bottom flanges are sealed with stainless-steel octagonal ring-type gaskets. In preliminary testing with a small vessel using these flanges, these gaskets were observed to have a relatively minimal dry leak rate compared to other options (i.e. carbon steel and/or oval ring). The leak rate was evaluated as 2.3×10^{-5} cm^3/s according to the ANSI-N14.5 specification for radioactive material transport packages after correcting from pressurized helium to air and leakage from 100 kPa to 1 kPa. However, measurements were found to be impacted by leakage in the plumbing lines, so results could only be used on a comparative basis.

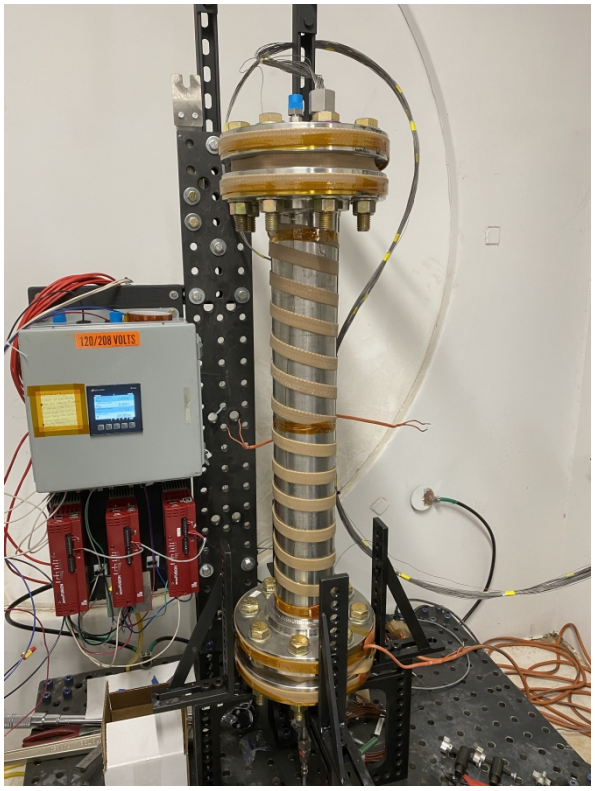

Figure 2-4 Photo of the pressure vessel used for the 5×5 DDA testing. Flexible heaters were wrapped around the pressure vessel to provide simulated decay heat.

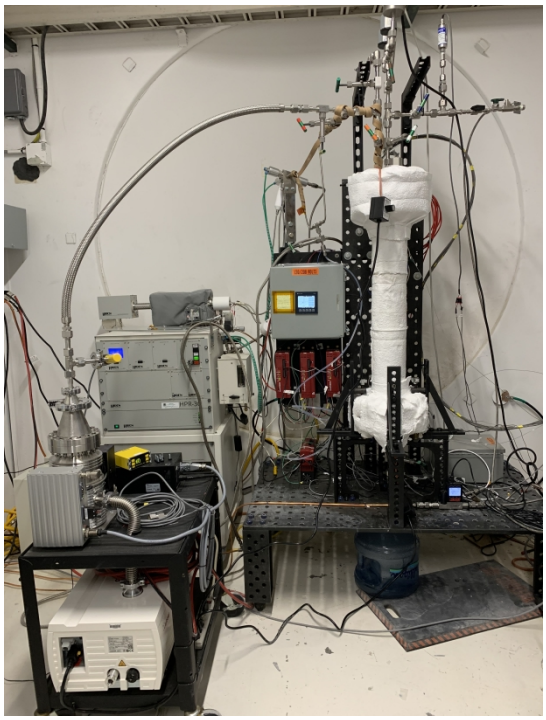

Figure 2-5 Photo of the complete drying test setup.

A diagram of the test setup including the pressure vessel is shown in Figure 2-6. Bellows-sealed valves form the boundaries to the main internal volume of the PV. The left PV isolation valve leads to the main vacuum pump line (green), consisting of a Leybold EcoDry 40+ scroll pump and a Leybold MAG W 300 iP turbo pump, as well as the mass spectrometer (purple), which uses an Edwards nXDS6i scroll pump and an Edwards nEXT070 turbomolecular pump to maintain a high vacuum within its sample chamber. The right PV isolation valve leads to the branch with the MKS and Setra pressure transducers as well as the helium pressurization line (red), while the bottom flange isolation valve is used for water filling and draining (blue).

Altogether, the vacuum-tight design minimizes leakage and allows for fine control of both sub-atmospheric pressures and high pressures up to 1000 kPa. The pressure vessel has been designed to minimize separation between assembly components and instrumentation through the use of blind flanges with penetrations for thermocouples (TCs) and instrumentation. Thermocouples are fed through a Viton packing in a compression fitting on the upper flange. This method of installation was permanent and prevented the replacement of gaskets or faulty TCs.

The pressure vessel was mounted on a stand comprised of fixture table components and steel framing. This stand also supported peripheral plumbing lines and provided a convenient location for the mass spectrometer sample block to minimize the length of the sample line tubing. With the length of the sample line minimized, the potential for fluid to condense is reduced, allowing the sampled gas to remain representative of the PV contents.

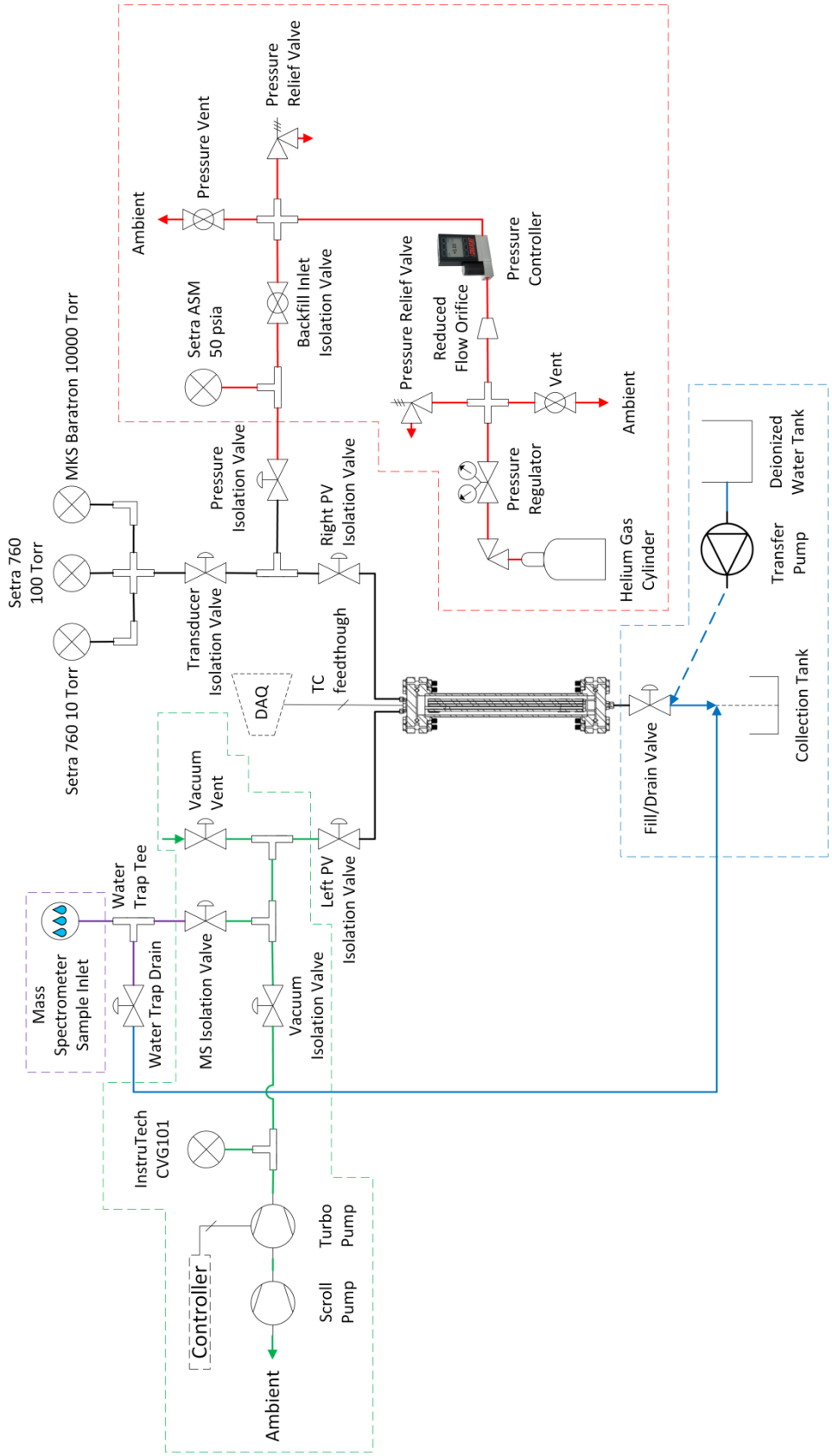

Figure 2-6 Diagram of pressure system.

2.4 Bulk Water Filling and Draining

The pressure vessel is filled with deionized water through a flexible hose connected to the bottom valve in the lower blind flange as shown in Figure 2-6. The system can be drained by the same plumbing by opening the fill/drain valve with further draining aided by pressurized blowdowns.

To determine the internal volume of the pressure vessel, a container of deionized water was weighed using a Mettler Toledo PBD655 bench platform (repeatability 1.3 g) and the water in the container was then poured into the vessel. The deionized water container was weighed following pours at two different fill levels – the first level was taken at the top of the fuel rod surrogates, while the second level was taken at the top of one of the VCR fittings on the top flange to determine the maximum volume of the pressure vessel. The container weights before and after the pour as well as the corresponding vessel water contents by weight at the two fill levels are listed in Table 2-1.

Table 2-1 Pressure vessel water volumes by weight at two different fill levels.

Event	Description	Container (kg)	Vessel Water (kg)	Vessel Volume (L)
Initial Weight	--	19.64	--	--
1st Pour	Free volume in fuel region	15.17	4.47	4.48
2nd Pour	Total, free volume in PV	14.47	5.17	5.18

For bulk water filling, about 4.54 kg of water was weighed using a Mettler Toledo MS12002TS precision balance (repeatability 0.01 g) and a tared container. This value of 4.54 kg was chosen to be between the 4.47 kg needed to fill to the top of the fuel surrogate rods and the 5.17 kg that would fill the entire pressure vessel. For the vacuum drying test with the empty guide tube, a transfer pump was used to fill the pressure vessel with water. The water, container, pump, and fill line were weighed before and after pumping the water into the pressure vessel. For the vacuum drying test with the poison rod, water was drawn into the PV by pulling a vacuum instead of using the transfer pump. The discrepancy in the pre-fill component weights between the two tests is largely due to the weight of the transfer pump. The weight of the water transferred into the pressure vessel is shown in Table 2-2. The volume of the burnable poison rod surrogate is 0.0478 L (2.914 in^3).

Table 2-2 Bulk water filling weights for determining water content pumped into pressure vessel.

Vacuum Drying Test	Pre-Fill Components (kg)	Post-Fill Components (kg)	Water in PV (kg)	Water in PV (L)
Empty guide tube	8.03	3.35	4.68	4.69
Poison rod	5.33	0.60	4.73	4.74

2.5 Instrumentation

This section will describe the instrumentation used to measure temperature and pressure during this test series, as well as instrumentation specific to moisture/water content measurement.

2.5.1 Thermocouples

Temperatures were measured using type-T thermocouples using the standard ASTM calibration specifications (ASTM, 2017). No additional calibrations were performed. A coordinate system was defined with an origin ($z = 0$) at the top of the bottom nozzle on the sub-assembly, where the rectilinear z-coordinate runs along the axial length of the pressure vessel towards the upper blind flange (see Figure 2-4). The thermocouples installed along the surfaces of the fuel rod surrogates (internal TCs) are shown in Table 2-3 with their data acquisition (DAQ) labels, while ambient TCs and those installed on the surface of the pressure vessel (external TCs) are listed in Table 2-4. The 0° angular direction is defined as the side

of the PV pipe near the strapping point on the mount. For the fuel rods, the 0° direction maintains this downward-facing (-*z*) reference for defining the clockwise direction.

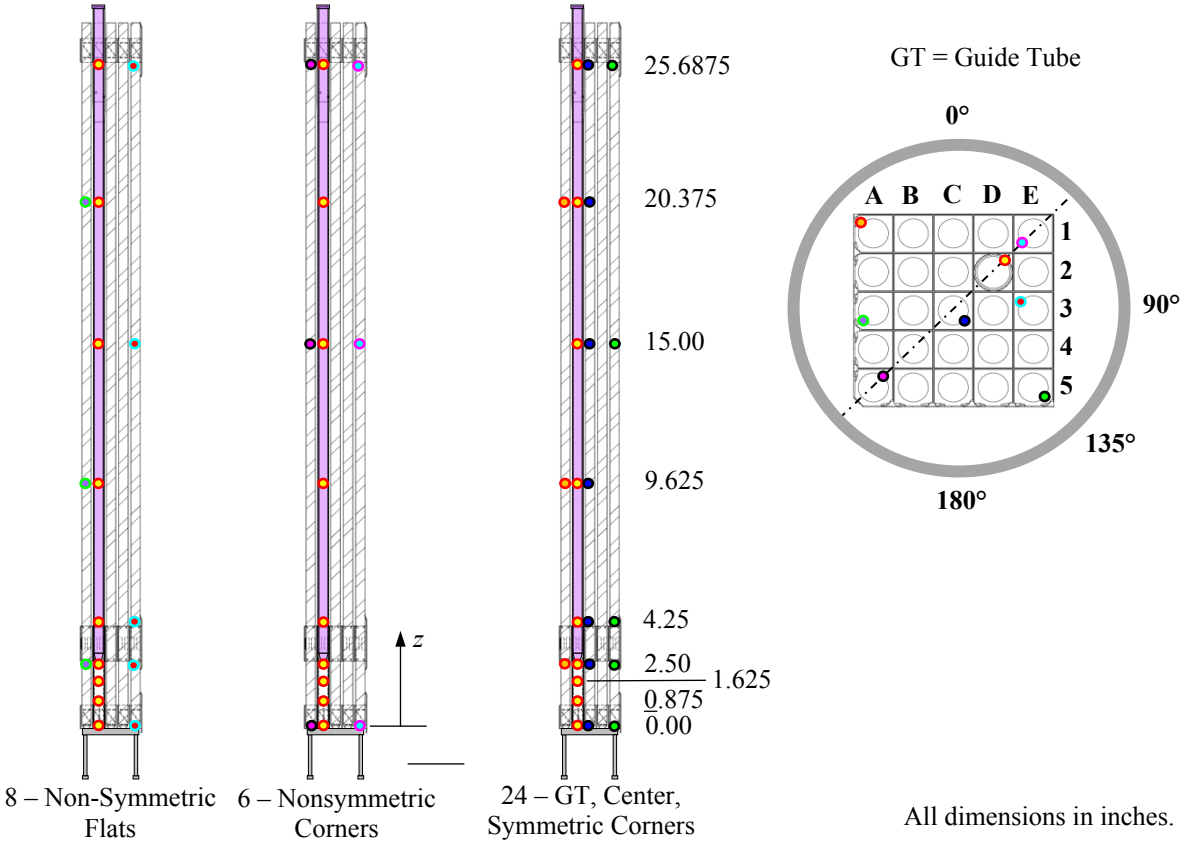

Figure 2-7 Diagram of thermocouple locations and assembly coordinate system.

Table 2-3 List of internal (Int.) thermocouples.

#	Type	Coordinate	*z* Position (in.)	Direction (Degrees)	DAQ Label
1	T	GT_D2	0.00	45°	GT_D2_0.00"
2	T	GT_D2	0.875	45°	GT_D2_0.875"
3	T	GT_D2	1.625	45°	GT_D2_1.625"
4	T	GT_D2	2.50	45°	GT_D2_2.50"
5	T	GT_D2	4.25	45°	GT_D2_4.25"
6	T	GT_D2	9.625	45°	GT_D2_9.625"
7	T	GT_D2	15.00	45°	GT_D2_15.00"
8	T	GT_D2	20.375	45°	GT_D2_20.375"
9	T	GT_D2	25.6875	45°	GT_D2_25.6875"
10	T	A1	2.50	315°	A1_2.50"
11	T	A1	9.625	315°	A1_9.625"
12	T	A1	20.375	315°	A1_20.375"
13	T	A3	2.50	225°	A3_2.50"
14	T	A3	9.625	225°	A3_9.625"

15	T	A3	20.375	225°	A3_20.375"
16	T	A5	0.00	45°	A5_0.00"
17	T	A5	15.00	45°	A5_15.00"
18	T	A5	25.6875	45°	A5_25.6875"
19	T	C3	0.00	135°	C3_0.00"
20	T	C3	2.50	135°	C3_2.50"
21	T	C3	4.25	135°	C3_4.25"
22	T	C3	9.625	135°	C3_9.625"
23	T	C3	15.00	135°	C3_15.00"
24	T	C3	20.375	135°	C3_20.375"
25	T	C3	25.6875	135°	C3_25.6875"
26	T	E1	0.00	225°	E1_0.00"
27	T	E1	15.00	225°	E1_15.00"
28	T	E1	25.6875	225°	E1_25.6875"
29	T	E3	0.00	315°	E3_0.00"
30	T	E3	2.50	315°	E3_2.50"
31	T	E3	4.25	315°	E3_4.25"
32	T	E3	15.00	315°	E3_15.00"
33	T	E3	25.6875	315°	E3_25.6875"
34	T	E5	0.00	135°	E5_0.00"
35	T	E5	2.50	135°	E5_2.50"
36	T	E5	4.25	135°	E5_4.25"
37	T	E5	15.00	135°	E5_15.00"
38	T	E5	25.6875	135°	E5_25.6875"
39	T	PV	-2.50	-	PV_Interior_BottomFlange
40	T	PV	2.50	-	PV_Interior_2.50"

The type-T TCs are intended to detect the presence of water by measuring sharp temperature changes that would be indicative of phase change during the vacuum drying procedure. The effective measurement range of type-T TCs runs from -270 to 400 °C. Under vacuum, the vapor pressure of the water inside water-retaining cavities will decrease and allow water to evaporate. As the rate of evaporation increases with decreasing pressures, the liquid temperature drops through evaporative cooling. Freezing may also occur if the enthalpy of fusion is exceeded near areas of restricted flow.

The external TCs in Table 2-4 are type-T and installed along the axial length of the pressure vessel at 0°, although some additional TCs are installed at 90°, 135°, and 180° as well. The ambient thermocouples are installed on the left side of the upright fixture table installation behind the pressure vessel (see Figure 2-5).

Table 2-4 List of external (Ext) and ambient (Amb) thermocouples.

#	Type	Surface	Location	*z* Position (in.)	Direction (Degrees)	DAQ Label
41	T	Ext.	PV	0.00	0°	PV_0°_0.00"
42	T	Ext.	PV	0.88	0°	PV_0°_.875"
43	T	Ext.	PV	1.63	0°	PV_0°_1.625"
44	T	Ext.	PV	2.50	0°	PV_0°_2.50"
45	T	Ext.	PV	4.25	0°	PV_0°_4.25"
46	T	Ext.	PV	9.63	0°	PV_0°_9.625"
47	T	Ext.	PV	15.00	0°	PV_0°_15.00"
48	T	Ext.	PV	20.38	0°	PV_0°_20.375"
49	T	Ext.	PV	25.69	0°	PV_0°_25.6875"
50	T	Ext.	PV	15.00	90°	PV_90°_15.00"
51	T	Ext.	PV	2.50	135°	PV_135°_2.50"
52	T	Ext.	PV	25.69	180°	PV_180°_25.6875”
53	T	Ext.	PV	34.08	-	PV_TopFlange
54	T	Ext.	PV	-4.33	-	PV_BottomFlange
61	T	Amb.	Mount	-5.00	-	Ambient_1_-5”
62	T	Amb.	Mount	14.50	-	Ambient_2_14.5”
63	T	Amb.	Mount	32.25	-	Ambient_3_35.25”

2.5.2 Pressure Measurement and Control

Multiple transducers are employed to provide data for various pressure ranges during the drying test. They are installed external to the PV on VCR fittings and separated with a series of isolation valves until measurement is needed.

An MKS Model 627F heated capacitance manometer rated at 1,333 kPa (10,000 Torr) is employed as an absolute pressure transducer. This manometer is meant to provide overarching pressure measurement for backfill pressurized operations (222 kPa) and vacuum operations (100 mTorr) in the pressure vessel. The corrosion- and fouling-resistant Inconel sensor measures pressure directly (independent of gas composition) and is maintained at a temperature of 45 °C after a warm-up period of 4 hours. The instrument has a resolution of 0.001% full-scale (FS) and accuracy of 0.12% of reading, and it is calibrated with a traceable reference standard. Measurements below 100 Torr were relegated to two additional vacuum transducers for higher accuracy.

Two Setra Vactron Model 760 capacitance monometers were used as absolute pressure transducers for operations under low vacuum. Two full-scale ranges of 1.33 and 13.3 kPa (10 and 100 Torr) were used, with resolutions of 0.01% FS, accuracies rated to ±0.15% of reading, and calibrations with standard traceable to the National Institute of Standards and Technology (NIST). This implies a minimum pressure measurement of 0.013 Pa (1 mTorr) for the test series as limited by the 1.33 kPa (10 Torr) manometer. These instruments are mounted vertically in a shared cross with the MKS transducer that is isolated from the pressure vessel via a bellows-sealed valve. The distance from the top flange and sample line heaters provided by this location mitigates the operating temperature constraint of 50 °C. Given proof pressures of 310 kPa (45 psia), the instruments were able to be exposed to the PV during the 160 kPa (23.2 psia) blowdown steps.

A Setra Model ASM high-accuracy pressure transducer is used to monitor pressure while backfilling the PV for drainage and blowdown. It has an accuracy of ±0.05% over a 345 kPa (50 psia) FS range, or ±0.10 kPa (±0.025 psia), and was calibrated to a primary standard traceable to NIST. The instrument interfaces with the pressure vessel via a pressure train leading from the top blind flange, which is separated from the manifold holding the main vacuum transducers. This branch includes a pressure relief valve, and it is isolated during vacuum drying tests to reduce leakage.

An Alicat Scientific PC-series single-valve pressure controller was used to set the fill pressure imparted to the pressure vessel from the helium cylinder. This controller has a NIST-traceable calibration to ±0.125% accuracy to the 1,034 kPa (150 psia) full-scale, with an operating range down to 0.5% FS. Repeatability of setpoint is specified at ±0.08% FS.

2.5.3 Water Content Measurement

Mass spectroscopy is a nontraditional method for measuring the relative moisture concentration in gas (i.e. parts per million by volume, ppm_v). In mass spectroscopy, a small sample stream (1 to 20 scm^3/min, where an scm^3 is a cubic centimeter of gas referenced at a standard temperature and pressure, depending on sample pressure) is ionized and drawn into a vacuum chamber through a quadrupole filter that influences how ionized species interact with the ion detector. Because mass spectroscopy draws a small sample flow, perturbations of the system pressure may be expected. Furthermore, adsorption and desorption of water on the small-bore stainless steel or glass capillary sample tubes can be an issue, especially as the sample flow rate drops with falling sample pressure. Heating the sample lines and quadrupole minimizes the problem, but it will still take several minutes of sample flow for equilibrium to be reached. For slowly changing transient operations expected in drying operation, the anticipated lags are expected to be manageable. With a properly designed inlet, the high temperature and the wide range of pressures inside the pressure vessel can be accommodated.

The Hiden Analytical HPR-30 is a 6 mm quadrupole mass spectrometer with a Faraday cup detector employed to analyze transient gas concentrations in gas samples from the pressure vessel obtained via a stainless-steel capillary tube with 0.173 in. (0.439 cm) inner diameter at two pressure ranges. This HPR-30 MS was used in previous testing (Salazar *et al.*, 2020), but the system was modified to allow for sampling between 10 and 100 kPa (1.45 to 14.5 psia) and between 1.33 and 13.3 kPa (10 to 100 Torr). The high-pressure range of 10 to 100 kPa (1.45 to 14.5 psia) was used for drying out the mass spectrometer with nitrogen and establishing a helium sampling background. A mid-pressure range of 1.33 to 13.3 kPa was used for vacuum drying tests. A low-pressure range of 0.05 to 0.5 kPa (0.375 to 3.75 Torr) from the previous HPR-30 configuration was also available, but the current test series did not allow for sampling at this range as the lowest pressures seen during vacuum drying were below the 0.375 Torr threshold.

The MS, shown in Figure 2-8, uses a scroll pump in combination with a turbo molecular pump to evacuate the internal volume and reduce the pressure within the spectrometer. This allows sample gases to flow into an ion source, which ionizes the molecular components of the sample gas.

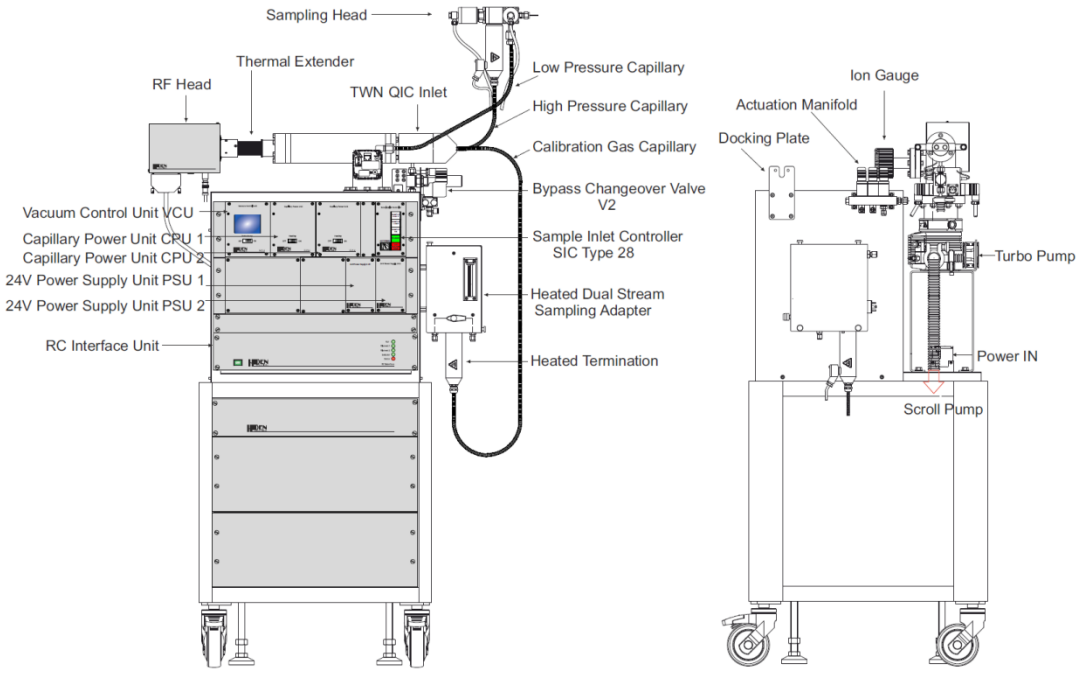

Figure 2-8 Hiden Analytical HPR-30 mass spectrometer system with a QIC dual-stage sampling head for measuring water content from the waterproof heater rod pressure vessel (Hiden Analytical Limited, 2018).

The ionized molecules are guided by a potential gradient between the ion source and ground to a quadrupole, which filters the molecules based on their mass-to-charge ratio *m*/*z* (amu/Coulomb). The quadrupole influences how the charged molecules are detected by the Faraday cup – the mass spectrometer outputs the number of counts of ion-detector collisions based on *m*/*z*. The relative concentrations of each molecular component can thus be calculated from the ion detector collision count peaks at each *m*/*z* value.

A given gas sample will have multiple peaks based on how the molecules are ionized (singly or doubly charged) and the presence of molecular isotopes. For each molecule, determining a relative concentration amounts to accounting for the major peak of that molecule, which is associated with the molecule's most common ionic species. For example, as shown in Figure 2-9, the three peaks associated with nitrogen come from singly-charged $^{28}N_2$ (28 amu/1 C = 28 amu/C), doubly-charged $^{28}N_2$ (28 amu/2 C = 14 amu/C), and singly-charged $^{29}N_2$ (29 amu/1 C = 29 amu/C). The 28 amu/C peak is the largest peak in the mass spectrum of nitrogen, so it is the peak used for quantification. A method could have been developed using all three peaks but the analysis would take longer to complete. Since the drying process is transient, a rapid method was needed to resolve temporal changes and only the major peaks for water, helium, nitrogen, oxygen, and argon were analyzed. The resulting analysis time for the method developed was about 45 seconds.

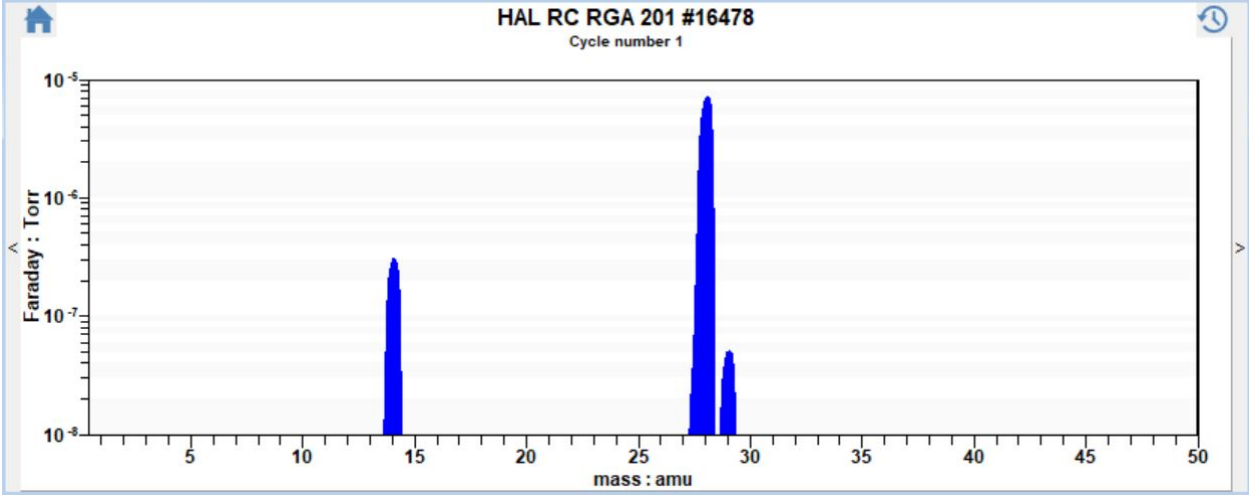

Figure 2-9 Mass spectrum of air showing the major peaks for nitrogen.

The amount of residual water detected will help define the effectiveness of the drying procedures implemented. An advantage of using an MS is that all other gaseous species are analyzed. For vacuum drying, the amount of air components can be used to evaluate the air leakage into the system. If used to monitor a commercial dry cask, an MS can also detect hydrogen generation that would indicate radiolysis or noble gas fission products (e.g. Kr-85 or Xe-137) that would indicate a leaking fuel rod.

The MS was calibrated to detect water content using a Michell DG2 two-stage dew point (DP) generator (-40 °C to +20 °C dew points). The generator uses a dry gas source such as ultra-high purity helium or air and generates a split stream that is mixed with moisture at a controlled temperature to generate a gas with a known dew point between -40 °C to +20 °C. The dew point of the calibration gas was verified by passing through a Michell S8000 chilled mirror hygrometer that can provide precision measurements to -65 °C dew point. The MS was calibrated for moisture concentrations between zero and 25,000 ppm_v using helium as the background gas. The calibration procedure was used to generate a relative sensitivity factor for water that is used to calibrate the mass spectrometer water content measurements to the chilled mirror hygrometer measurements. This calibration procedure is described in great detail in the FY20 waterproof heater rod testing report (Salazar *et al.*, 2020).

The result of the calibration conducted for this test series is shown in the linear regression in Figure 2-10. The relative sensitivity factor was calculated to be 0.2137, taken from the slope of the linear regression. The intercept was previously defined as the detection limit of the mass spectrometer. However, the apparent outlier at the high ppm_v water content may have affected the regression calculation, resulting in a negative intercept. The linear regression had a coefficient of determination of $R^2 = 0.9971$ and a standard error of 36.1 ppmv. The 95% confidence interval for the regression, based on the *t*-statistic of 1.975 and the standard error, was ±71.3 ppm_v. The standard deviation of the difference between the corrected HPR-30 and S8000 data was ±169.0 ppm_v.

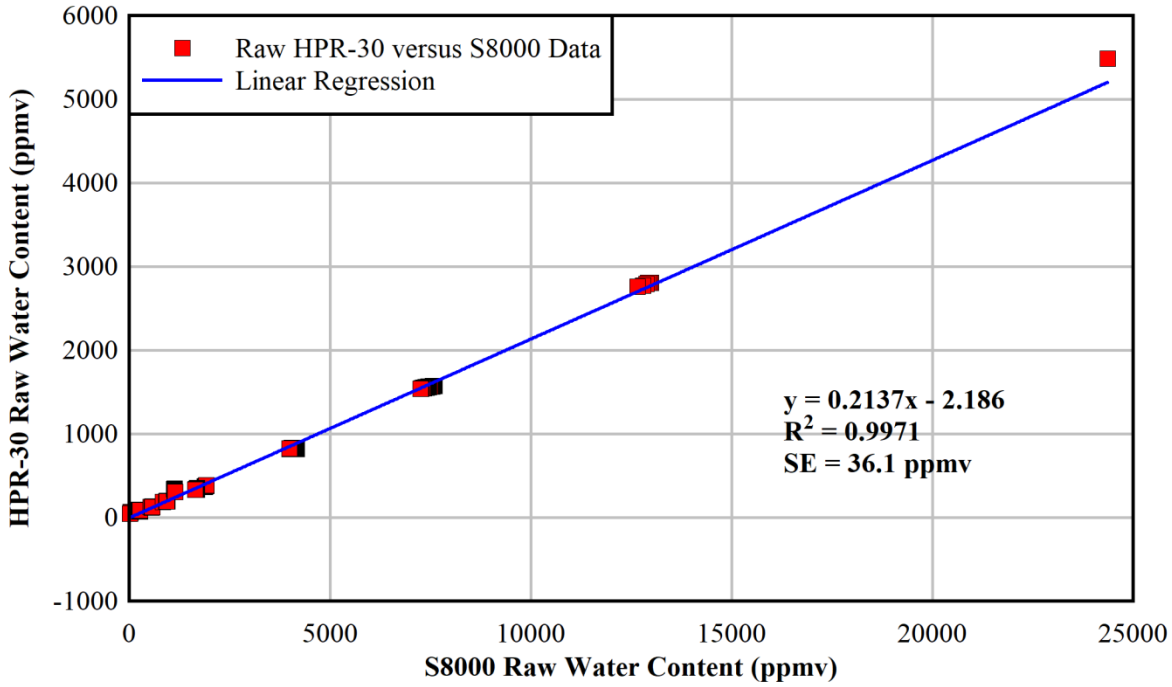

Figure 2-10 Linear regression for determining the relative sensitivity factor for water in a helium background when calibrating the HPR-30 mass spectrometer with respect to the S8000 chilled mirror hygrometer.

2.6 Power Control

The electrical power supplied to each heating element on the pressure vessel was controlled using four digital silicon-controlled rectifiers (SCR) labeled A through D. These were used to maintain the desired temperatures in the PV and guide tube and to have them remain within safe operating margins. The device software provided digital power setpoints to each SCR that was controlled based on external power feedback from a calibrated diagnostic unit (APlus) installed on the 120 VAC power supply. Diagnostic measurements from the APlus were available from SCRs A – C by connecting their power lines to the three available ports. On-board power information from SCR D was fed directly to the DAQ.

Table 2-5 lists the instruments used for power control and measurement, and Figure 2-11 shows the power control setup. Given the 627 W rating and 219 °C temperature limit of the flexible heaters, 10-amp fuses were installed in the circuit in the event that the heaters shorted during the tests. The full-scale settings for SCR control were defined as 1,000 watts, 120 volts, and 8.333 amps. The SCRs shared the same ground as the power source. A power conditioner was used to stabilize the power signals to the SCRs and impart more predictable power fluctuations during the test.

A flexible heater was installed in the mass spectrometer inlet line (the purple line in Figure 2-6) and was controlled manually using a built-in control panel. This was done to reduce the potential for moisture condensation and maintain a representative PV sample.

Table 2-5 List of power control equipment.

Description	Manufacturer	Model
Digital SCR AC Power Controller	Control Concepts	uF1HXLGI-130-P1RSZ
Power Monitor with System Analysis	Camille Bauer	APlus
24 VDC Power Supply	Black Box	MDR-60-24
Power Conditioner	Eaton	PowerSure 800
Flexible Heaters with Stripped Leads	Omega	SRT202-060LSE
Flexible Heater with Percentage Controller	Omega	HTWC101-006

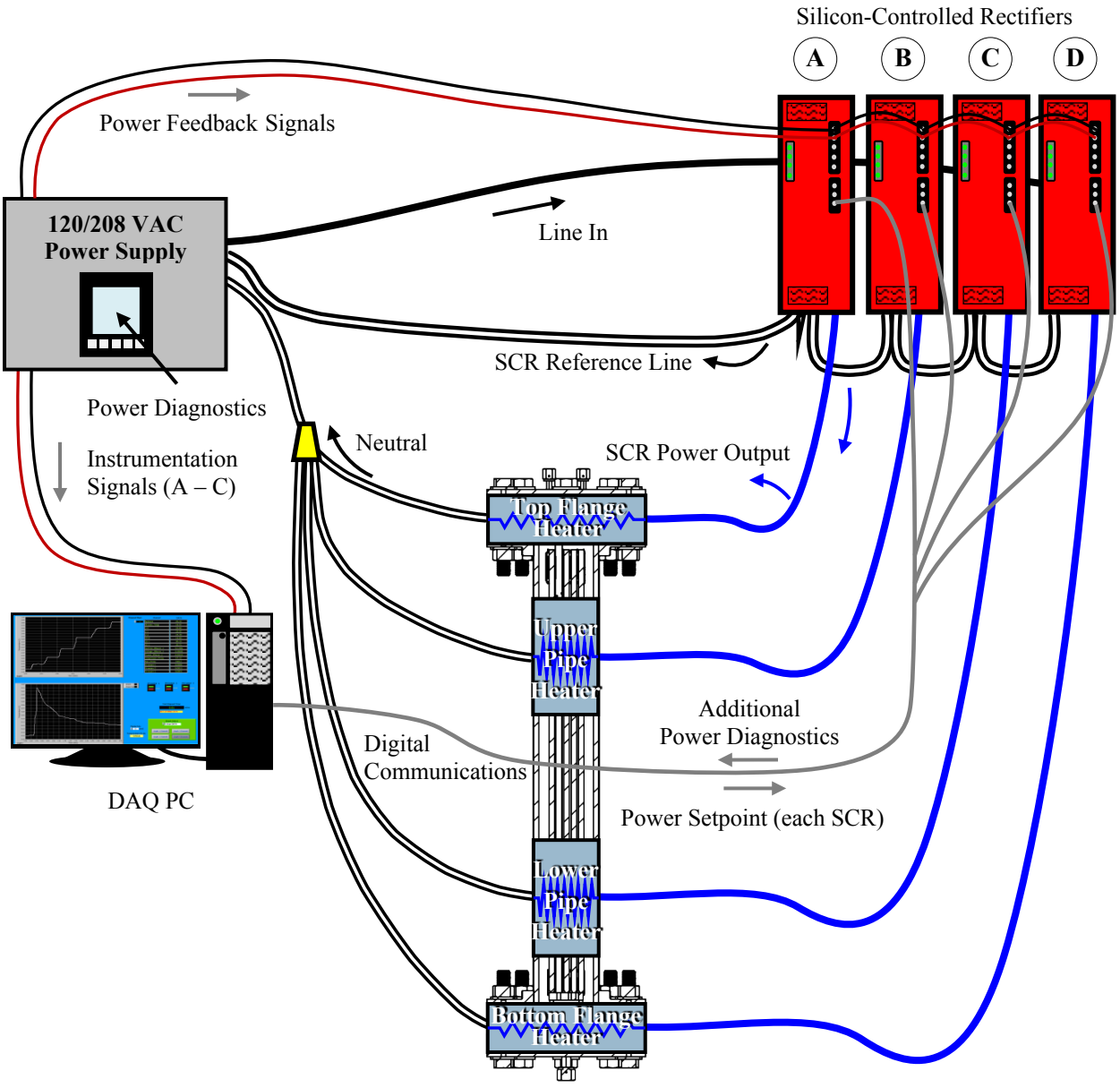

Figure 2-11 Diagram of the power control setup for the external heaters on the PV.

3 PRELIMINARY TEST RESULTS

3.1 Data from the High Burnup Demonstration Project

The temperature and pressure history for the drying and backfill portions of the HBDP was used as guidance for operating the DDA during testing. Figure 3-1 shows the temperature (top) and pressure (bottom) histories of the HBDP. The relative axial position of the temperature data labeled in the legend are shown by matching colored lines overlain on the inset HBDP vertical cross-section. Transient pressure data was not available to the authors. The pressure history presented in the plot was reconstructed from the available description and details as recorded in the High Burnup Test Report (EPRI, 2019). No details were provided on vacuum hold points during the vacuum drying procedure. This procedure is therefore represented as a dashed straight line between known pressures at the start and end of the drying procedure. The dryness test started at a pressure of 0.055 kPa (0.041 Torr) at 13.8 hours and rebounded to 0.13 kPa (0.97 Torr) after 30 minutes. The cask was then backfilled with helium to 102 kPa then evacuated to 10 kPa before finally being backfilled with helium to 220 kPa.

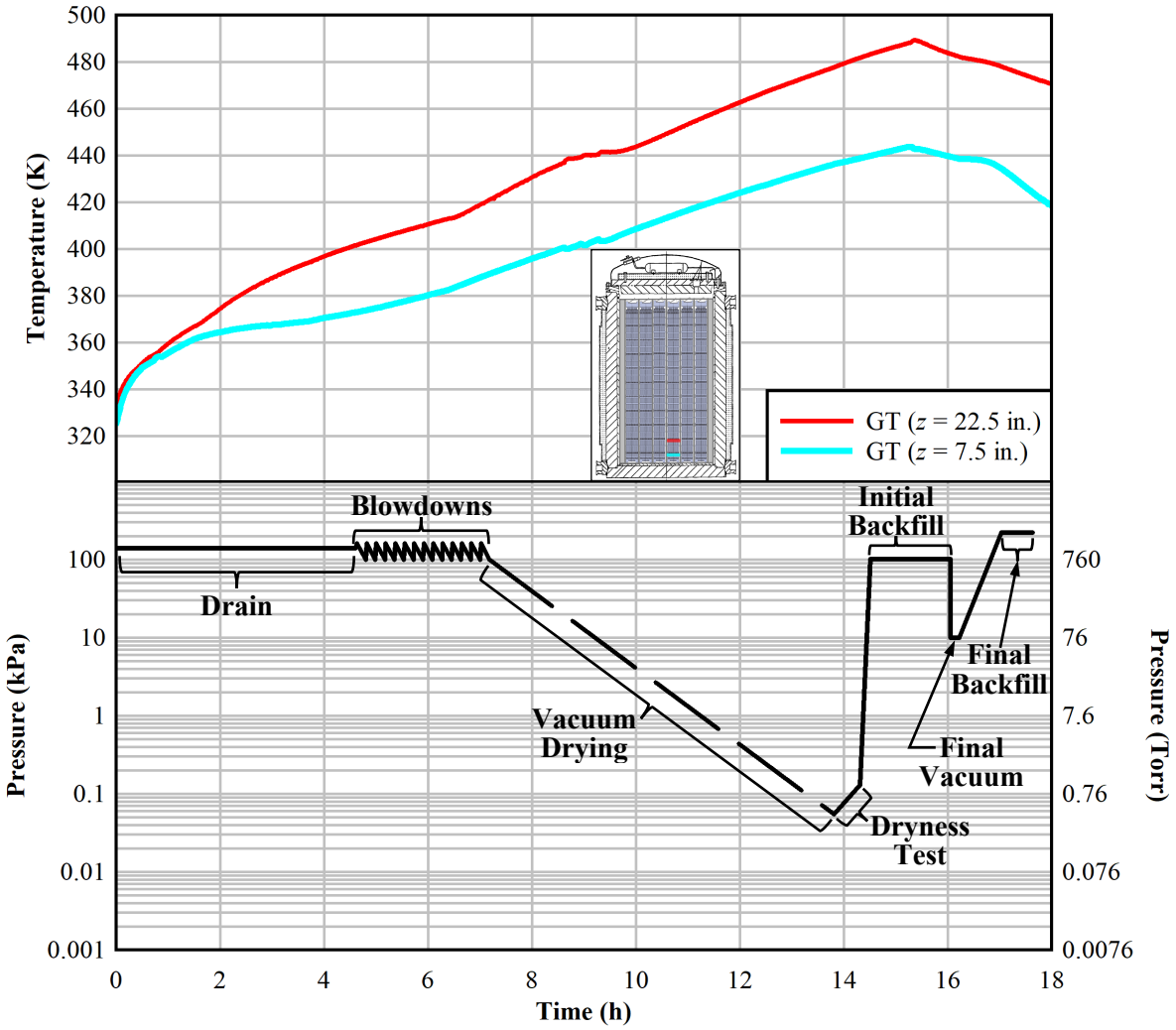

Figure 3-1 Temperature (top) and pressure (bottom) histories during drying of the High Burnup Demonstration Project.

The peak temperature at the upper portion of the region of interest (z = 22.5 inches) was a bit over 480 K and the peak temperature at the lower region (z = 7.5 inches) was just over 440 K. The time for performing the entire drying operation for the HBDP was just under 18 hours. These temperature and pressure histories from the HBDP serve as the template for the testing with the DDA described in the next section.

3.2 Dashpot with Poison Rod Test

3.2.1 Temperature and Pressure Histories

Figure 3-2 shows the corresponding temperature (top) and pressure (bottom) histories of the DDA during the drying test conducted with a poison rod insert on August 25, 2021. The overall time scale is compressed by a factor of two compared to the HBDP shown in Figure 3-1. The relative axial position of the temperature data labeled in the legend are shown by matching colored lines overlain on the inset DDA vertical cross-section.

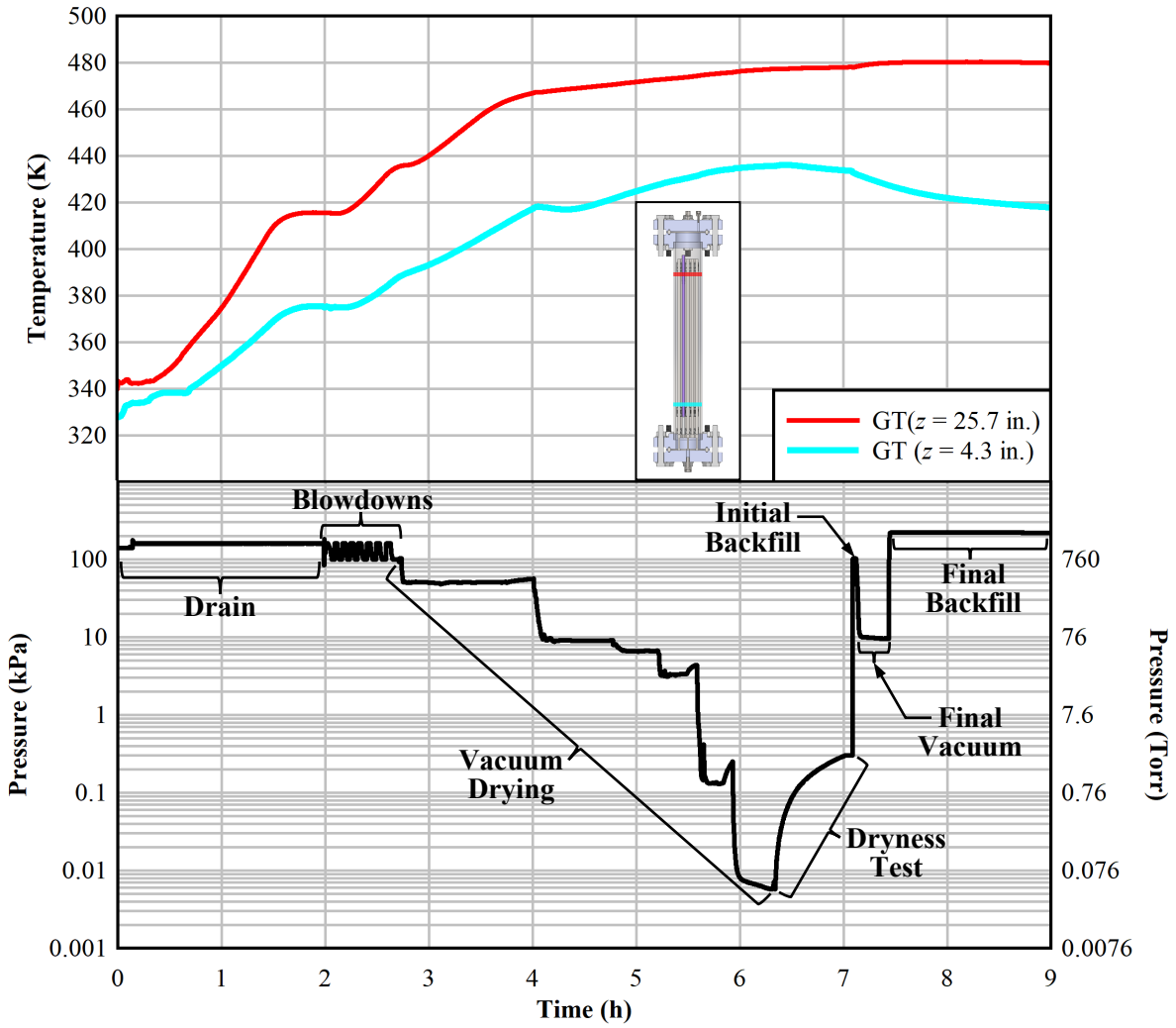

Figure 3-2 Temperature (top) and pressure (bottom) histories during simulated drying of the DDA with a poison rod insert on 08/25/21.

The transient pressure data shows all the details of the test progession with the initial vacuum hold of 50 kPa (380 Torr) at 2.75 h, the next hold of 10 kPa (76 Torr) at 4 h on down to the final hold of 0.007 kPa (0.05 Torr) at about 6 h. The final vacuum hold rebounded to 0.30 kPa (2.3 Torr) just after 7 h. The vessel was then backfilled with helium to 103 kPa, evacuated to 10 kPa (76 Torr) and held for 20 minutes. The final backfill to 222 kPa was implemented at about 7.4 h.

The peak temperature at the upper portion of the region of interest (z = 25.7 inches) was 480 K and the peak temperature at the lower region (z = 4.3 inches) was just under 440 K. The time for performing the entire operation was about 9 hours.

Figure 3-3 shows the evolution of guide tube temperatures over time during the drying test with the poison rod present for the five highest elevations. Of particular interest is the temperature measured at the lowest position at z = 0.0 inches. The guide tube thermocouple at this location measured two sharp drops in temperature coincident with changes to the vacuum holds. The first decrease in temperature is a small depression at the initial vacuum hold of 50 kPa (380 Torr) at 2.75 h. The temperature recovered quickly and did not last the duration of the vacuum hold. The second sharp temperature decrease is much more significant at the hold of 10 kPa (76 Torr) at 4 h. The decrease in temperature lasted the better part of an hour. These temperature decreases are clear evidence of signifiacant water evaporation near the bottom of the DDA.

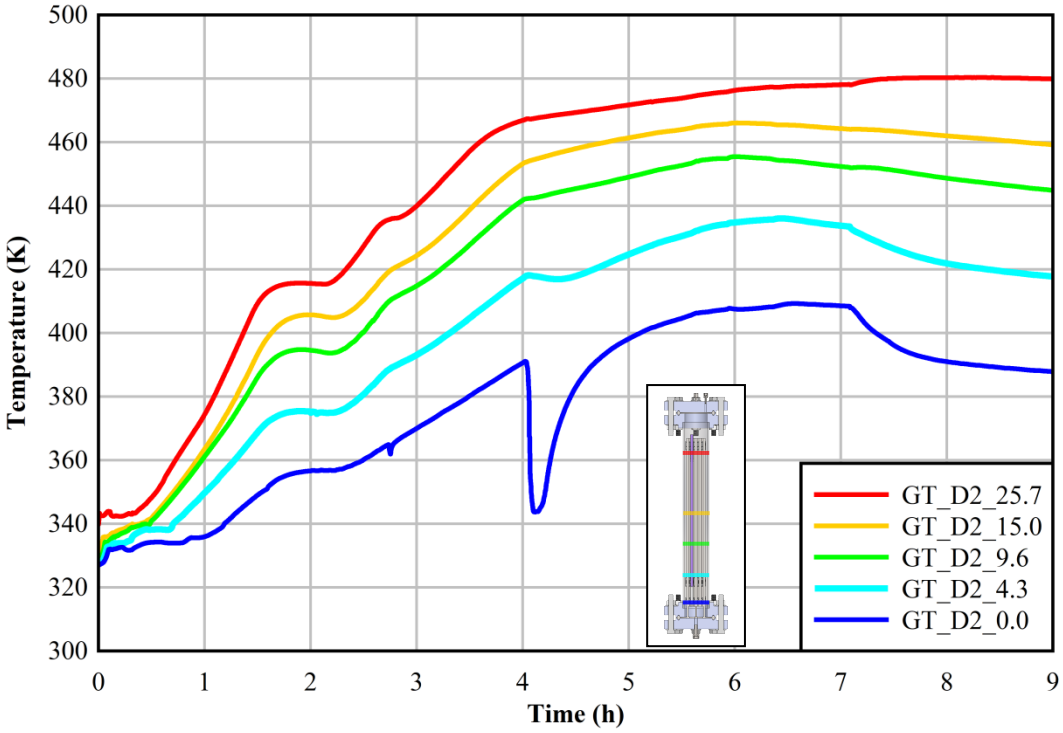

Figure 3-3 Guide tube temperatures versus time during simulated drying of the DDA with a poison rod insert on 08/25/21.

Figure 3-4 shows temperature contours of the DDA at times before and after the second vacuum hold of 10 kPa (76 Torr) during the drying test with the poison rod inserted.

Figure 3-5 shows an enlarged view of the DDA temperature contours. The temperature depression at the vacuum hold of 10 kPa is clearly evident in temperature contours of the right-hand image at t = 4.07 h.

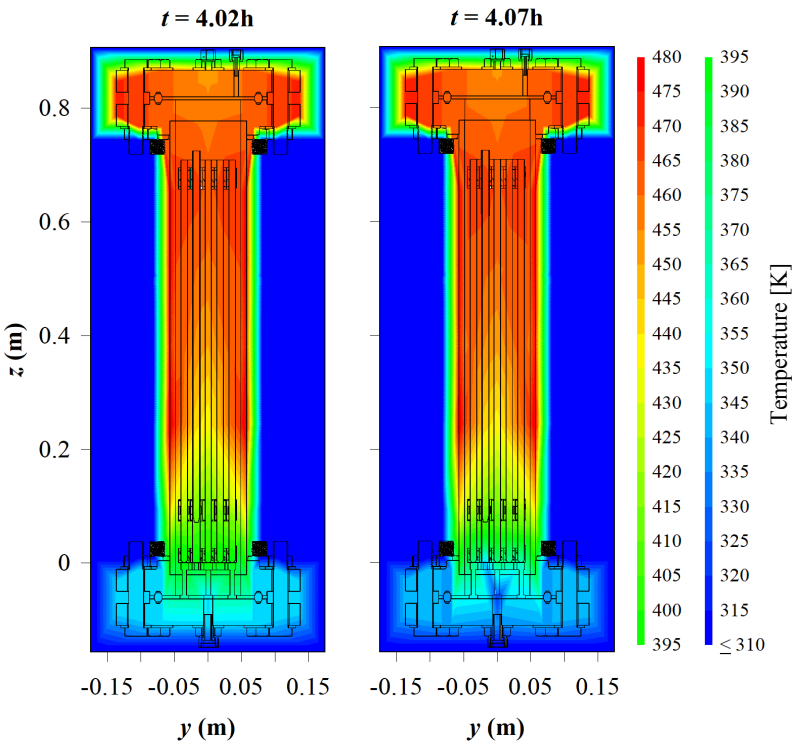

Figure 3-4 **Temperature contours of the DDA with a poison rod insert at times before and after the observed temperature drop during drying on 08/25/21.**

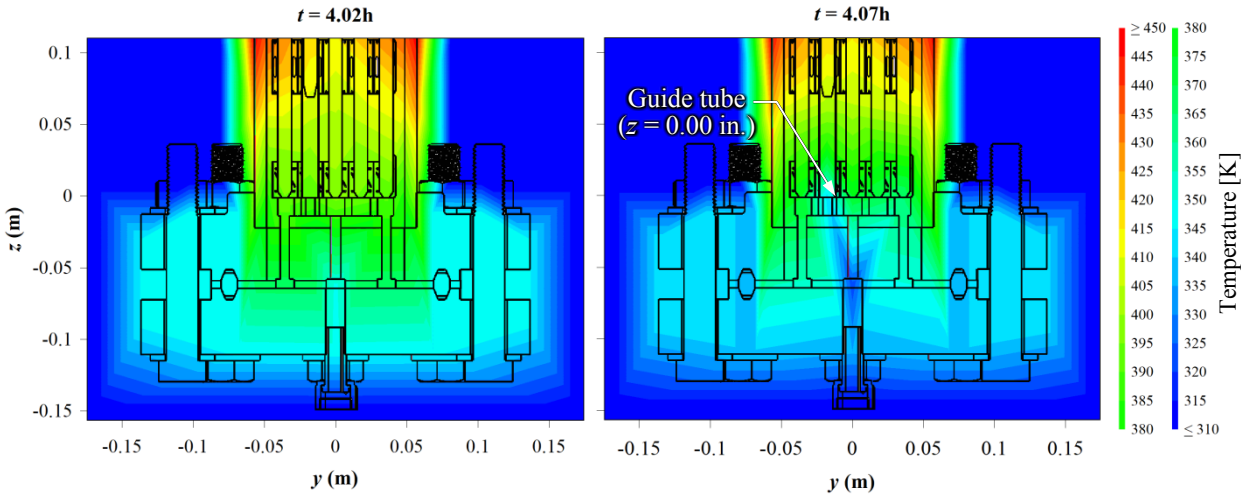

Figure 3-5 **Enlarged view of the bottom of the DDA with a poison rod insert at times before and after the observed temperature drop during drying on 08/25/21.**

3.2.2 Water Content

Table 3-1 shows the weight of the measured initial water inside the DDA plus the container used to hold the water. It also shows the weight of the water recovered (plus the container) from the helium blowdown procedure for the DDA with a poison rod insert. The difference between the weight of the water and container before filling and after recovery from the helium blowdown procedure gives a measure of the water remaining in the DDA after the helium blowdowns. These measurements indicate that there was about 70 ml of water left in the vessel that needed to be removed by the drying procedure.

Table 3-1 DDA measured initial water content versus recovered water for determining water remaining in DDA after helium blowdown procedure for the DDA with a poison rod insert.

Weight of Water + Container Before Filling (kg)	Recovered Water + Container (kg)	Water Remaining in DDA (kg)	Water Remaining in DDA (L)
5.32	5.25	0.070	0.070

The following section summarizes the mass spectrometer data collected from the DDA test series with the poison rod in place conducted over the time period from August 25, 2021 to August 31, 2021. No mass spectrometer data is reported for the DDA test series without the poison rod in place that was initiated on August 20, 2021 because an air leak compromised the samples.

The mass spectrometer has three independent inlets for sampling gas within three different pressure ranges. The three inlet sampling ranges were 100 to 10 kPa, 13.3 to 1.33 kPa, and 0.5 to 0.05 kPa. Since the pressure vessel was at 140 kPa during the drain step and rapidly changed between 160 and 100 kPa during the helium blowdown steps, the mass spectrometer could not sample from the pressure vessel during the drain and helium blowdown steps. Additionally, problems were encountered when attempting to sample the vessel at the lowest pressure using the 0.5 to 0.05 kPa sampling inlet. In order to accommodate these constraints and provide a measure of dryness, cycling of the pressure in the vessel down to 10 kPa for sampling followed by pressurization with helium to the 220 kPa hold point continued for several more days past the “Final Backfill” shown in Figure 3-2.

Table 3-2 shows the results of mass spectrometer gas sampling, as ppm_v, from the DDA during the subsequent 10 kPa holds at various test dates. The reported values are the averages of 3 to 5 measurements after a steady state measurement was achieved. It took about five minutes to reach steady state. Also shown in Table 3-2 is the calculated dew point of the gas at the both the sampling and hold pressures. The dilution factor is the factor by which the measured moisture concentration would be expected to drop if the vessel was completely dry prior to pressurization.

The sample from 8/25/2021 was taken during the vacuum drying procedure during the final vacuum hold shown on Figure 3-2 after the 102 kPa initial helium backfill at about 7 hours. At over 150,000 ppm_v, the moisture content is very high. While the 13 °C dew point at the sample pressure suggests there was no liquid water present during sampling, the 55 °C dew point at the hold pressure suggests water condensation during the high-pressure hold. Some of the lines connecting the pressure transducers to the vessel were not heated allowing moisture to condense and perhaps drain back into the heated vessel. Following the sampling on 8/25/2021, the vessel was pressurized with helium to the 220 kPa final backfill hold.

Table 3-2 Mass spectrometer water content data across a series of vacuum isolation holds at approximately 10 kPa and subsequent helium re-pressurizations for the DDA with a poison rod insert.

Sampling Date	High Pressure Hold, P_{Hold} (kPa)	Vessel Sampling Pressure P_{Sample} (kPa)	Dilution Factor P_{Hold}/P_{Sample}	Measured Water Content (ppm_v)	Sample Pressure Dew Point (°C)	Hold Pressure Dew Point (°C)
8/25	102.0	9.8	10.4	152,179	12.9	54.7
8/26	220.0	9.7	22.7	85,377	4.3	58.7
8/27	220.0	9.7	22.7	79,902	4.0	57.3
8/30	220.0	9.5	23.2	9,580	-20.6	18.3
8/31	220.0	9.5	23.2	4,740	-27.7	7.6

The following day, the vessel pressure was dropped to the 10 kPa hold and sampled. The moisture content dropped to 85,000 ppm_v but the dew point at the hold pressure remained high again indicating condensation of water. The vessel was repressurized to 220 kPa, left overnight and sampled by the same procedure the next day on 8/27/2021. The moisture content dropped marginally, and the hold pressure dew point remained high indicating the continued presence of condensed water.

The procedure was repeated two more times. The sampling on 8/30/2021 measured an eight-fold drop in moisture concentration but only about a third of the dilution factor. The hold pressure dew point dropped to 18 °C suggesting the absence of liquid water. After the final sampling on 8/31/2021 the moisture content dropped a factor of two to 4,700 ppm_v and the dew point dropped to 8 °C indicating no liquid water was present during the hold but the unheated lines are prone to water adsorption.

3.3 Empty Dashpot Test

3.3.1 Temperature and Pressure Histories

Figure 3-6 shows the temperature (top) and pressure (bottom) histories of the DDA during the drying test conducted on August 20, 2021 without a poison rod inserted. The overall time scale is again compressed compared to the HBDP. The relative axial position of the temperature data labeled in the legend are shown by matching colored lines overlain on the inset DDA vertical cross-section. The transient pressure data shows all the details of the test progession with the initial vacuum hold of about 50 kPa (380 Torr) at 2.6 h, the next hold of about 10 kPa (76 Torr) at 3.6 h on down to the final hold of 0.002 kPa (0.015 Torr) at about 5.3 h. The final vacuum hold rebounded to 0.037 kPa (0.28 Torr) at 6 h. The vessel was then backfilled with helium to 102 kPa, evacuated to 10 kPa (76 Torr) and held for 20 minutes. The final backfill to 222 kPa was implemented at about 6.5 h.

The peak temperature at the upper portion of the region of interest (z = 25.7 inches) was about 472 K and the peak temperature at the lower region (z = 4.3 inches) was just under 418 K. The time for performing the entire operation was about 6.6 hours.

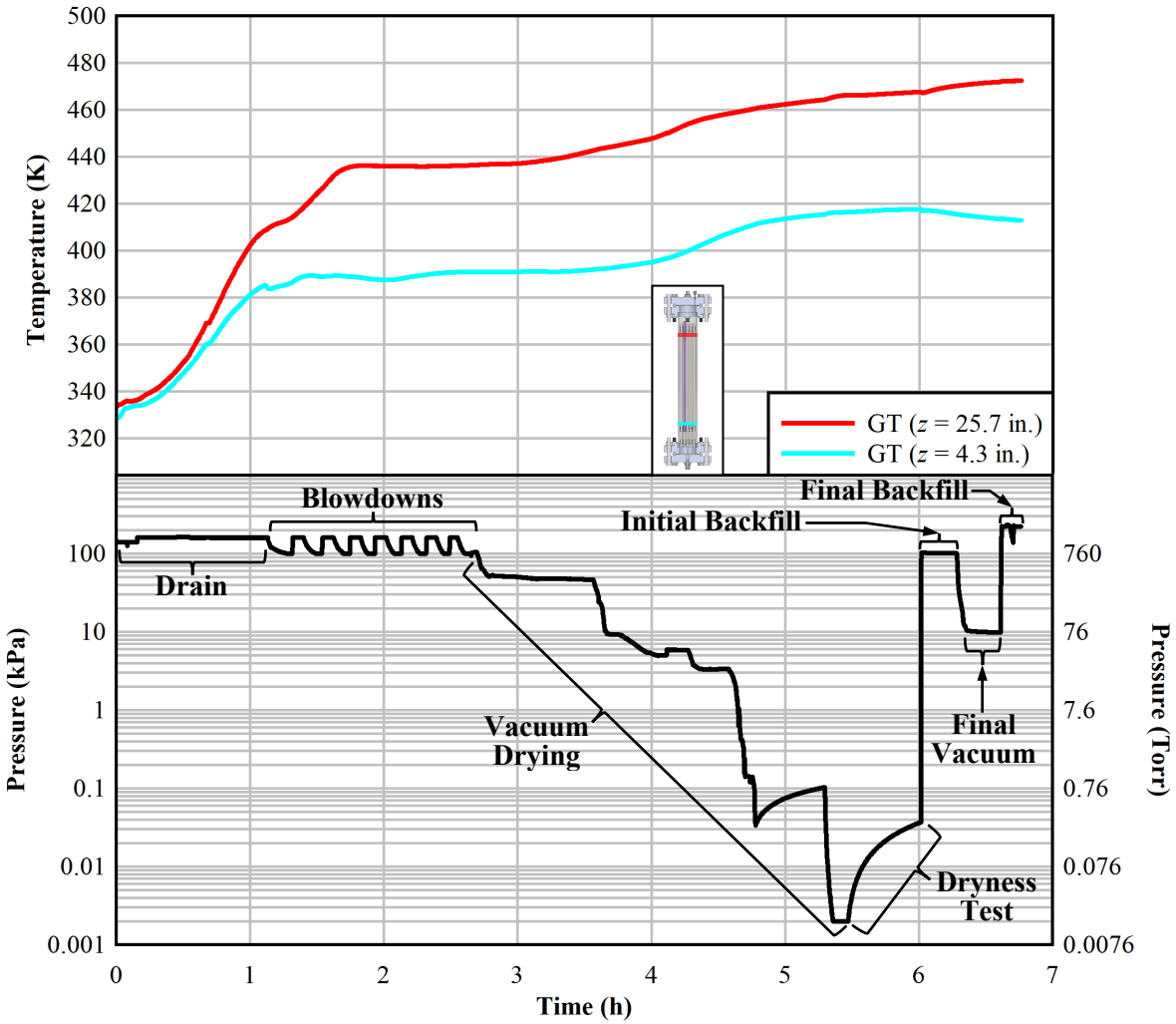

Figure 3-6 Temperature (top) and pressure (bottom) histories during simulated drying of the DDA with an empty guide tube on 08/20/21.

Figure 3-7 shows the evolution of guide tube temperatures over time during the drying test without the poison rod inserted for five elevations. Of particular interest is the temperature measured at the lowest position at z = 0.0 inches. Unlike the test with the poison rod present, there were no sharp decreases in temperature observed at the initial vacuum hold of 50 kPa (380 Torr) at 2.6 h or at the second hold of 10 kPa (76 Torr) at 3.6 h. Repeat testing is needed to determine if the presence of the poison rod has a bearing on the observed behavior.

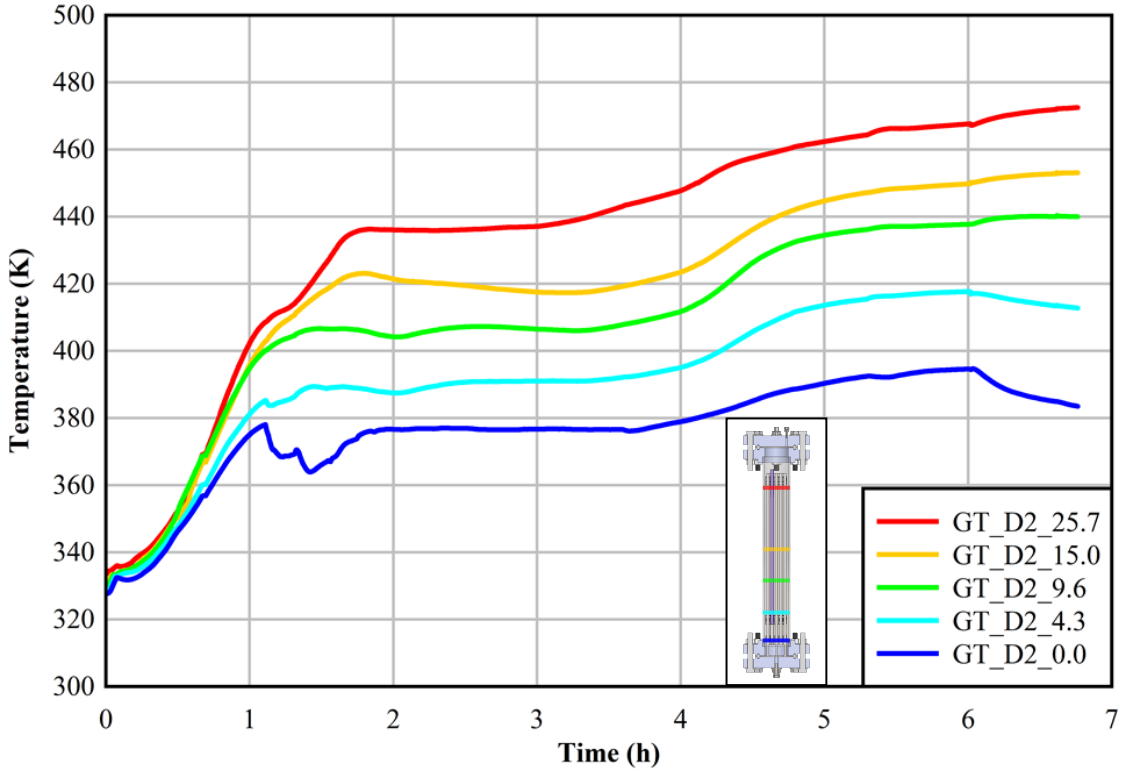

Figure 3-7 Guide tube temperatures versus time during simulated drying of the DDA with an empty guide tube on 08/20/21.

3.3.2 Water Content

Table 3-3 shows the weight of the measured initial water inside the DDA plus the container used to hold the water. It also shows the weight of the water recovered (plus the container) from the helium blowdown procedure for the DDA without a poison rod insert. The difference between the weight of the water and container before filling and after recovery from the helium blowdown procedure gives a measure of the water remaining in the DDA after the helium blowdowns. These measurements indicate that there was about 150 ml of water left in the vessel that needed to be removed by the drying procedure. No mass spectrometer data is reported for the DDA test series without the poison rod in place that was initiated on August 20, 2021 because an air leak compromised the samples.

Table 3-3 DDA measured initial water content versus recovered water for determining water remaining in DDA after helium blowdown procedure for the DDA without a poison rod insert.

Weight of Water + Container Before Filling (kg)	Recovered Water + Container Weight (kg)	Water Remaining in Pressure Vessel Weight (kg)	Water Remaining in Pressure Vessel Volume (L)
5.30	5.15	0.150	0.150

4 SUMMARY

Validation of the extent of water removal in a dry spent nuclear fuel storage system based on drying procedures used at nuclear power plants is needed to close existing technical gaps. Operational conditions leading to incomplete drying may have potential impacts on the fuel, cladding, and other components in the system. A general lack of data suitable for model validation of commercial nuclear canister drying processes necessitates additional, well-designed investigations of drying process efficacy and water retention. Scaled tests that incorporate relevant physics and well-controlled boundary conditions are essential to provide guidance to the simulation of prototypic systems undergoing drying processes.

4.1 Dashpot Drying Apparatus

A new small-scale pressure vessel with a 5×5 fuel assembly and axially-truncated Pressurized Water Reactor (PWR) hardware was created to simulate commercial vacuum drying processes. This test assembly, known as the Dashpot Drying Apparatus (DDA), was built to focus on the drying of a single PWR dashpot and surrounding fuel. Drying operations were simulated for two preliminary tests with the DDA based on the pressure and temperature histories observed in the High Burnup Demonstration Project (HBDP). One test was conducted with an empty guide tube. The other test was performed with a poison rod surrogate inserted into the top of the guide tube. These tests proved the capability of the DDA to mimic commercial drying processes on a limited scale and detect the presence of bulk and residual water. Furthermore, pressure remained below the 3 Torr rebound criterion for the final evacuation step in the drying procedure.

The instrumentation, power control, and mass spectrometer of the DDA functioned as designed. However, limitations on the maximum temperature of the external flexible heaters somewhat limited peak cladding temperatures compared to the HBDP. In addition, portions of the pressure and vacuum trains were not actively heated and likely acted as cold traps for water retention. Measurements with the mass spectrometer were probably biased by these cold traps functioning as water sources during the tests and therefore do not provide any meaningful analysis. Planned improvements to the DDA include the installation of higher temperature external heaters and self-regulating heat trace cables along all wetted lines in the pressure and vacuum trains.

4.2 Future Work

Work is planned to continue testing with the improved DDA as outlined above. This testing is intended to provide repeatability and further refinement of residual water measurements. The data and operational experience gained from the DDA test series is expected to guide and improve the next drying test, which is based on a partially-submersible, full-scale PWR fuel assembly.

Termed the Advanced Drying Cycle Simulator (ADCS), this next drying test series is currently planned to bridge the prototypic complexity of the HBDP and the focused scale of the DDA. This new apparatus will use a prototypic 17×17 commercial PWR skeleton populated with submersible electrically resistive heaters and will feature a specialized test rod. The fuel length would be prototypic and generate realistic temperature gradients, all while maintaining the intricate features of the guide tubes and grid spacers.

A pressure vessel concept for housing the specialized assembly is shown in Figure 4-1. The PV is comprised of two sections of nominal 14 in. pipes joined by welded flanges with ring-type joints, where the smaller pipe at the bottom is designed specifically to accommodate thermocouple compression fittings. Water would fill and drain through the welded siphon tube welded to the upper portion of the top pipe. This is meant to better represent a commercial canister system, where no lower drain is possible. The mass spectrometer would have a direct sampling port near the top of the pressure vessel and would be placed near other penetrations for electrical power feeds and pressure.

A removable test rod can be used for internal pressure monitoring or representations of breached rods. Heaters would comprise the majority of rod positions in the skeleton and be of uniform electrical

resistance. The test rod would be located at the very center of the assembly and serve as a flexible, replaceable testing component fed through an opening in the pressure vessel.

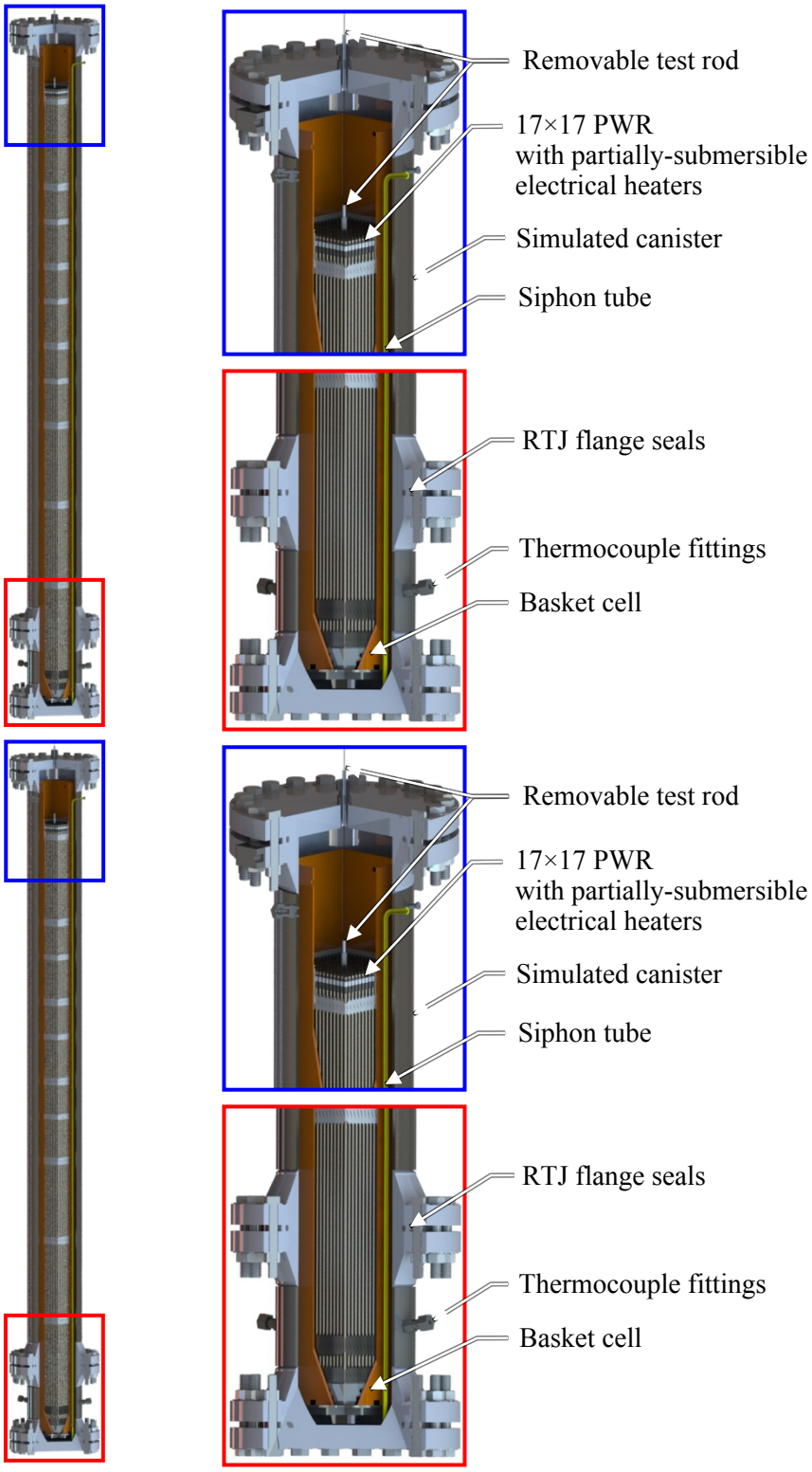

Figure 4-1 **Schematic of the Advanced Drying Cycle Simulator using a prototypic-length 17×17 PWR test assembly.**

5 REFERENCES

ASTM International (2016). Standard Guide for Drying Behavior of Spent Nuclear Fuel (C1553-16). ASTM Book of Standards Volume 12.01. West Conshohocken, PA.

ASTM International (2017). Standard Specification for Temperature-Electromotive Force (emf) Tables for Standardized Thermocouples (E230/E230M-17). ASTM Book of Standards Volume 14.03. West Conshohocken, PA.

Bryan, C. R., Jarek, R. L., Flores, C., & Leonard, E. (2019). Analysis of Gas Samples Taken from the High Burnup Demonstration Cask (SAND2019-2281). Sandia National Laboratories. Albuquerque, NM.

Colburn, H. A. (2021). Small Scale Drying: FY21 Interim Report. PNNL-31749. Pacific Northwest national Laboratory, Richland, WA.

EPRI. High Burnup Dry Storage Research Project Cask Loading and Initial Results (2019). Technical Report 3002015076. Palo Alto, CA.

Fort, J. A., Richmond, D. J., Jensen, B. J., & Suffield, S. R. (2019). High-Burnup Demonstration: Thermal Modeling of TN-32B Vacuum Drying and ISFSI Transients (PNNL-29058). Pacific Northwest National Laboratories. Richland, WA.

Hanson, B. D., & Alsaed, H. A. (2019). Gap Analysis to Support Extended Storage and Transportation of Spent Nuclear Fuel: Five-Year Delta (SFWD-SFWST-2017-000005, Rev 1; PNNL-28711). Pacific Northwest National Laboratory. Richland, WA.

Hiden Analytical Limited (2018). TWN QIC Dual Stage Sampling Head manual (HA-085-850). Warrington, United Kingdom.

Knight, T. W. (2019). Experimental Determination and Modeling of Used Fuel Drying by Vacuum and Gas Circulation for Dry Cask Storage (NEUP 14-7730). University of South Carolina. Columbia, SC.

Knoll, R., & Gilbert, E. (1987). Evaluation of Cover Gas Impurities and their Effects on the Dry Storage of LWR (Light-Water Reactor) Spent Fuel (PNL-6365). Pacific Northwest National Laboratory. Richland, WA.

Nuclear Regulatory Commission (2002). Westinghouse Technology Manual (ML023040131). Washington, D.C.

Nuclear Regulatory Commission (2010). Standard Review Plan for Spent Fuel Dry Storage Systems at a General License Facility (NUREG-1536). Washington, D.C.

Salazar, A., Pulido, R. J. M., Lindgren, E. R., & Durbin, S. G. (2019). Advanced Concepts for Dry Storage Cask Thermal-Hydraulic Testing (SAND2019-11281 R). Sandia National Laboratories. Albuquerque, NM.

Salazar, A., Lindgren, E. R., Fasano, R. E., Pulido, R. J. M., & Durbin, S. G. (2020). Development of Mockups and Instrumentation for Spent Fuel Drying Tests (SAND2020-5341 R). Sandia National Laboratories, Albuquerque, NM.

This page is intentionally left blank.

APPENDIX A MECHANICAL DRAWINGS

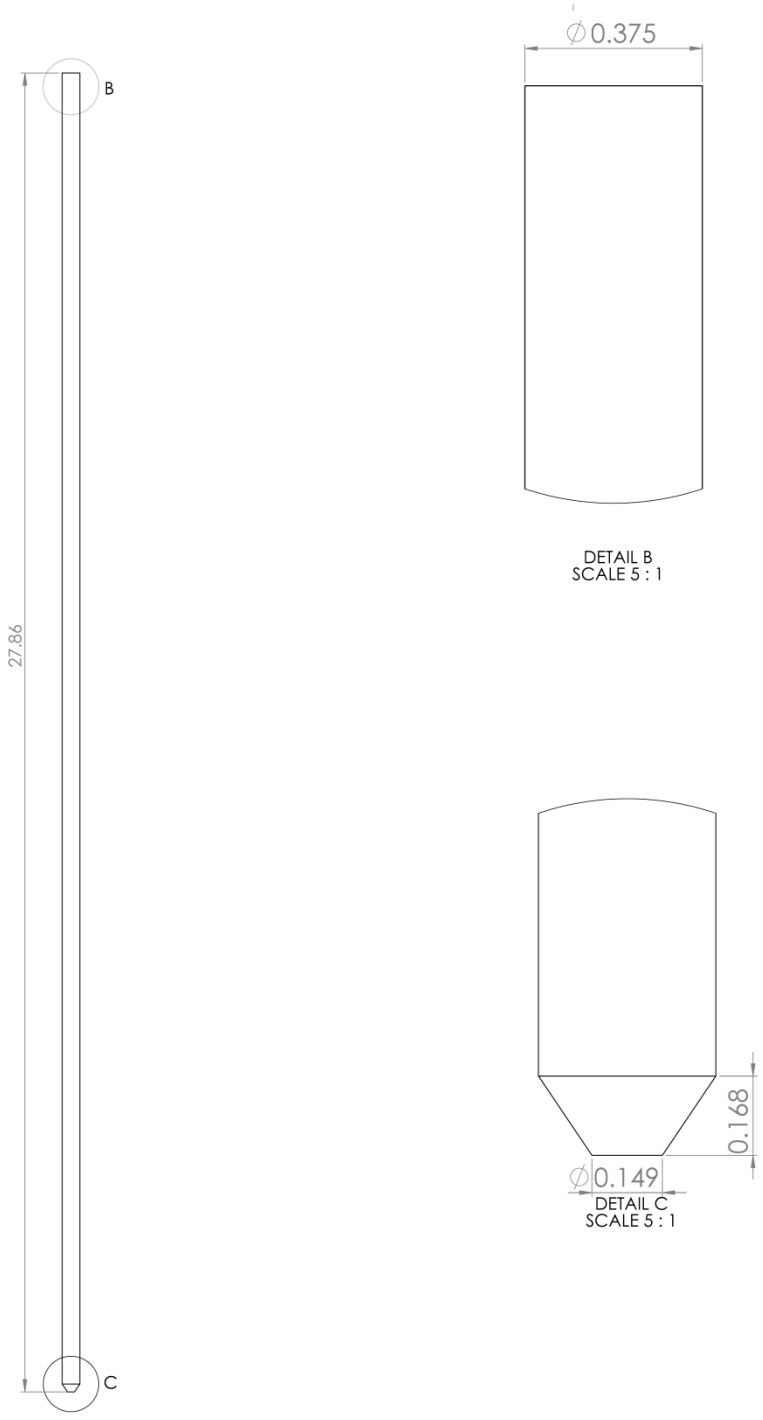

Figure A-1 Fuel rod surrogate.

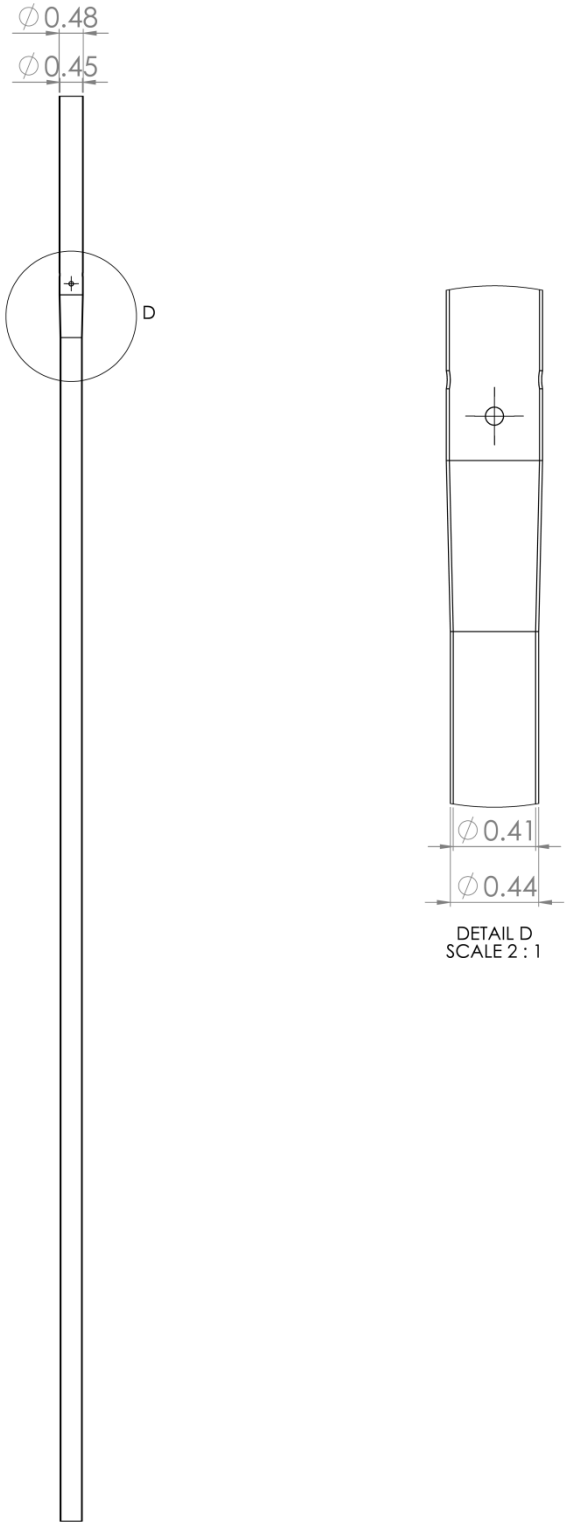

Figure A-2 Guide tube.

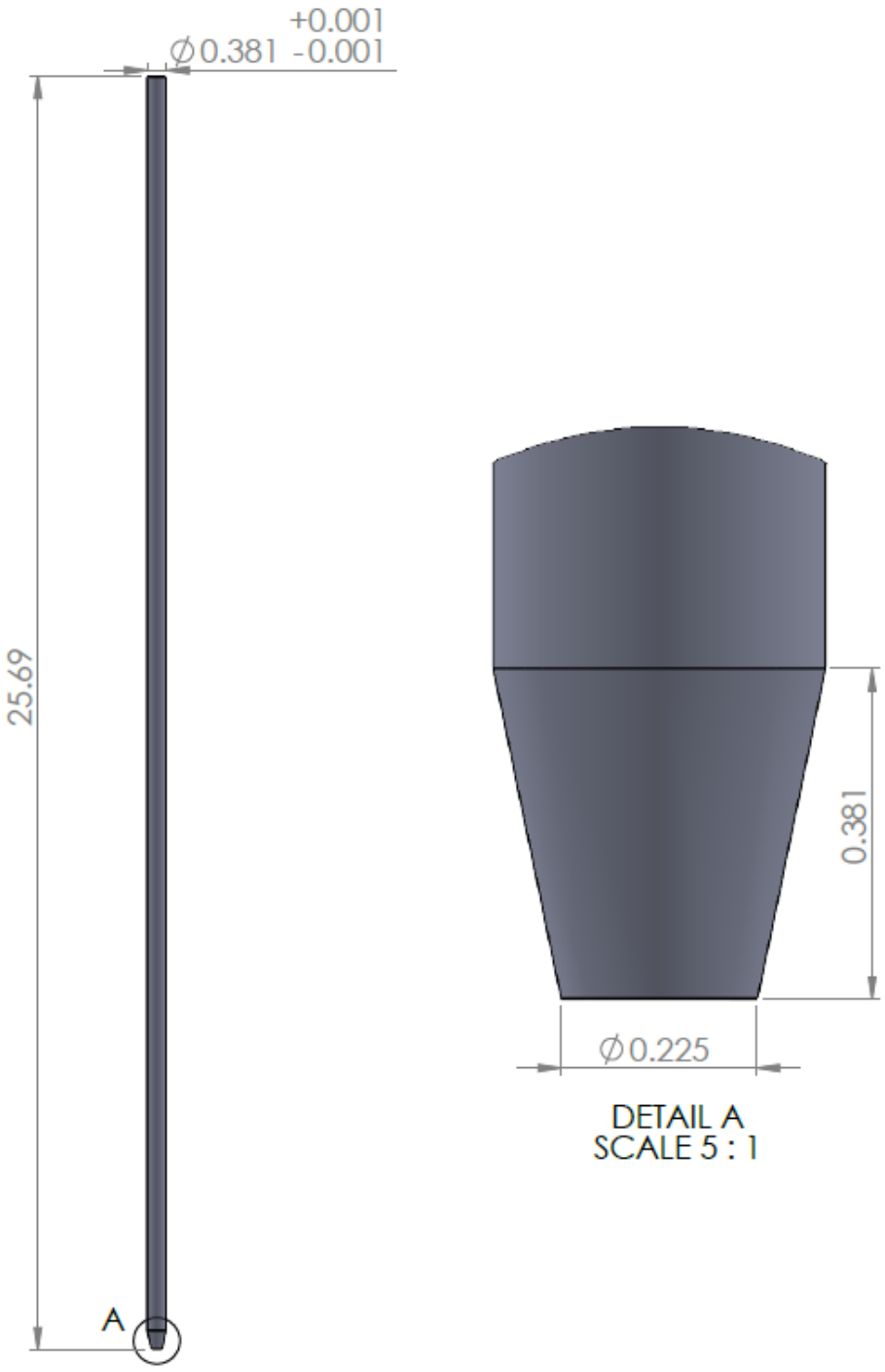

Figure A-3 Poison rod surrogate.

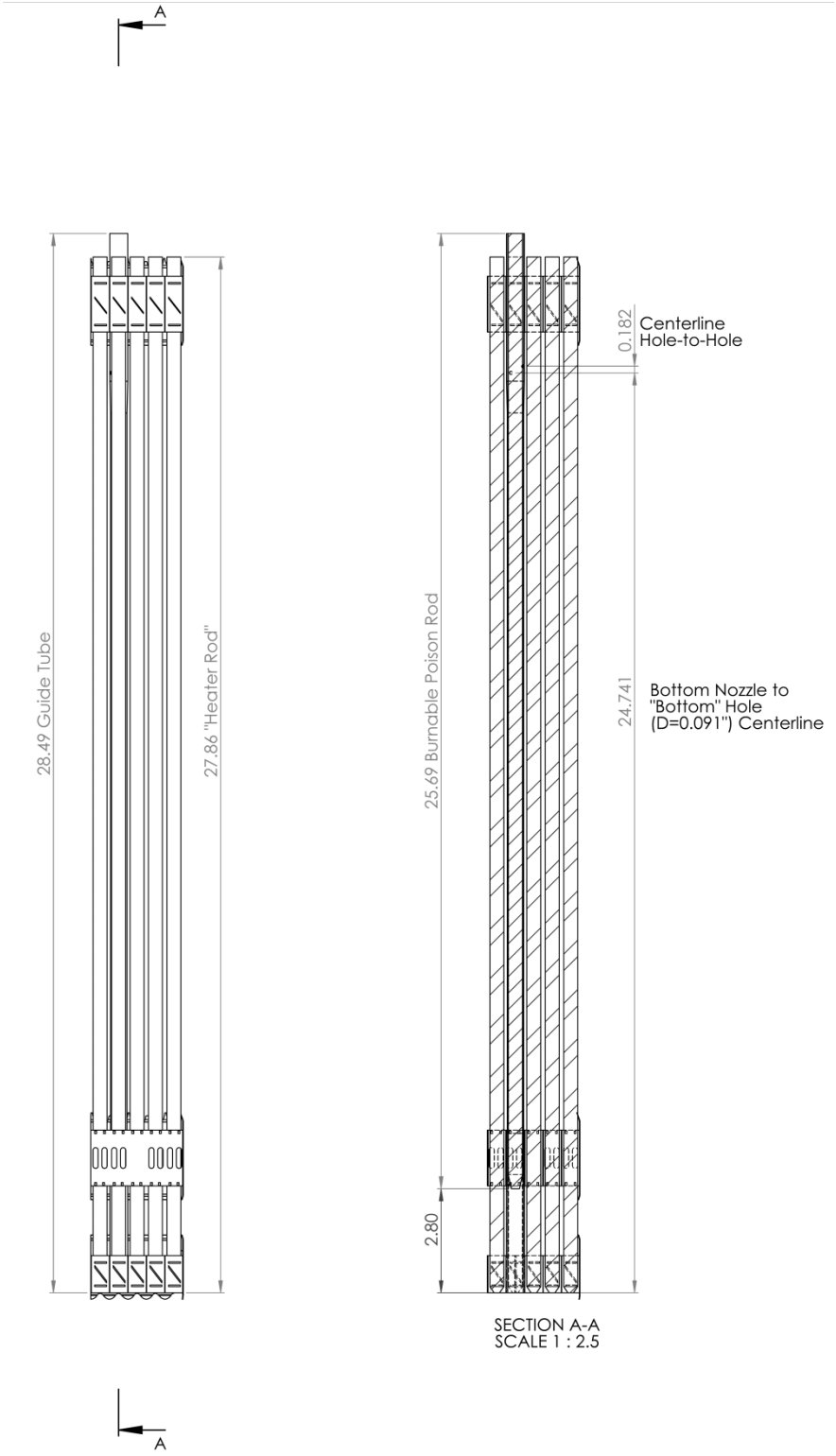

Figure A-4 Assembly side views.

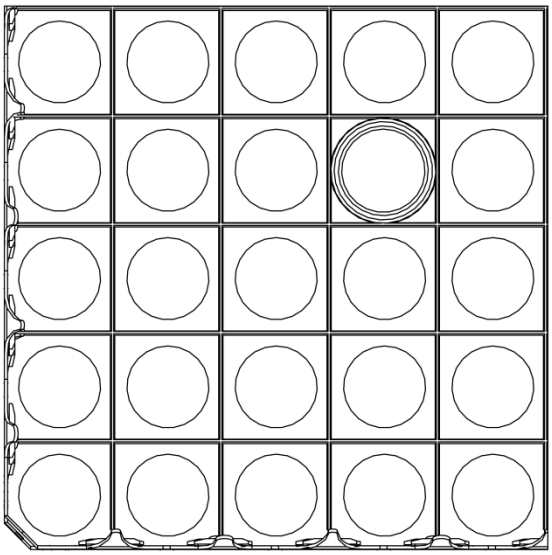

Figure A-5 Assembly cross section.

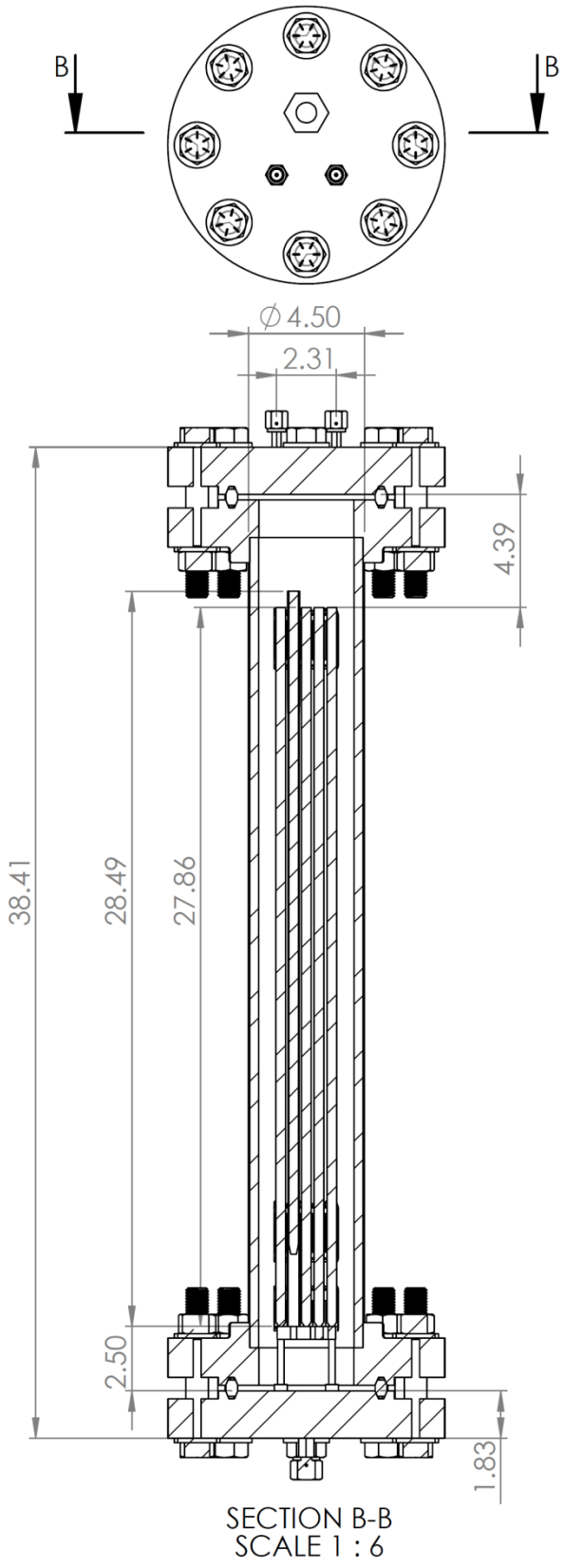

Figure A-6 Schematic of pressure vessel.

Sandia National Laboratories